Palaeogeography, Palaeoclimatology, Palaeoecology 381–382 (2013) 33–46

Contents lists available at SciVerse ScienceDirect

Palaeogeography, Palaeoclimatology, Palaeoecology

journal homepage: www.elsevier.com/locate/palaeo

Carbon isotope excursions in Boreal Jurassic–Cretaceous boundary sections and their correlation potential

Oksana S. Dzyuba [a,*], Olga P. Izokh [b], Boris N. Shurygin [a]

[a] Trofimuk Institute of Petroleum Geology and Geophysics, Siberian Branch of RAS, Acad. Koptyug av., 3, Novosibirsk 630090, Russia
[b] Sobolev Institute of Geology and Mineralogy, Siberian Branch of RAS, Acad. Koptyug av., 3, Novosibirsk 630090, Russia

ARTICLE INFO

Article history:
Received 30 July 2012
Received in revised form 29 March 2013
Accepted 9 April 2013
Available online 24 April 2013

Keywords:
Jurassic–Cretaceous boundary
Siberia
Carbon and oxygen isotopes
Belemnites

ABSTRACT

The Jurassic–Cretaceous (J–K) boundary is one of the most problematic points on the geological timescale. The boundary is not defined by a Global Stratotype Section and Point (GSSP) because of the absence of well-defined (by significant faunal turnover), widely correlatable biostratigraphic levels to fix the base of the Berriasian. A distinct earliest Berriasian positive carbon isotope excursion is identified in the Boreal marine carbonate (belemnites) carbon records from the Maurynya River (Northern Urals) and the Nordvik Peninsula (northern East Siberia). The excursion is found within the top part of the upper Volgian *Craspedites taimyrensis* ammonite Zone, slightly above the J–K boundary, which was established by palaeomagnetic data. Because a significant positive $\delta^{13}C$ shift was also observed immediately above the J–K boundary in the Tethyan Guppen-Heuberge pelagic-carbonate section (Switzerland), this positive carbon isotope event can be regarded as a useful marker for a Panboreal and Boreal–Tethyan correlation of J–K boundary beds. This $\delta^{13}C$ excursion is interpreted as a record of increased rates of organic carbon burial. The $\delta^{13}C$ data obtained previously for the upper Volgian and Ryazanian in different Boreal regions are also analysed in this paper. Other well-documented carbon isotope excursions with less global significance allow the creation of a composite carbon-isotope curve for Boreal regions that characterises the upper Volgian and Ryazanian in detail.

© 2013 Elsevier B.V. All rights reserved.

1. Introduction

1.1. Scope of the study

Carbon isotope variations have been widely used for palaeoclimatological and palaeoecological reconstructions and for precise correlation in many intervals of Earth's history. Previous studies of carbon isotope variations in Jurassic–Cretaceous (J–K) carbonate sections of Tethyan regions have not shown any significant excursions around the J–K boundary (Weissert and Channell, 1989; Weissert and Lini, 1991; Emmanuel and Renard, 1993; Savary et al., 2003; Tremolada et al., 2006; Michalík et al., 2009; Grabowski et al., 2010; Žák et al., 2011). The ranges of $\delta^{13}C$ values during this interval do not exceed 1‰ and are often 0.5‰. The one exception is the Guppen-Heuberge section (Switzerland), where the $\delta^{13}C$ values in the interval of calpionellid zones A and B vary within a relatively wide range from −0.2 to +1.6‰ (Weissert and Mohr, 1996). According to Michalík et al. (2009), carbon-isotope curves from bulk carbonate samples of J–K boundary sequences around the world show smooth trends resulting from equilibrated rates of bio-productivity and organic matter burial.

Reconstructions of carbon-isotope curves for northern palaeobasins with terrigenous sedimentation are based on the analysis of sedimentary organic matter and/or mollusc shell material, especially belemnites, which are best preserved in Boreal sections. Isotope geochemical studies of the J–K boundary interval of Boreal sections are still in progress. Stable isotope data have been collected from many Volgian and/or Ryazanian sections, where the J–K transition beds are poorly represented or absent: Speeton in England (Price et al., 2000); Helmsdale in Scotland (Nunn and Price, 2010); Janusfjellet and Knorringfjellet in central Spitsbergen (Hammer et al., 2012); Gorodischi, Kashpir and Marievka on the Russian Platform (Ruffell et al., 2002; Gröcke et al., 2003; Price and Rogov, 2009); Yatriya in Western Siberia (Price and Mutterlose, 2004); and Boyarka in Eastern Siberia (Nunn et al., 2010). In many instances, either detailed carbon isotope records have not been presented (e.g., Podlaha et al., 1998) or the studied sections have no detailed biostratigraphic subdivision (e.g., Ditchfield, 1997). Compared with the studied Tethyan carbonate sections, the Boreal sections are characterised by significant carbon isotope excursions on the $\delta^{13}C$ curves. Thus, if the excursions from different Boreal sections are shown to be isochronous, Boreal palaeobasins could be more suitable than Tethyan basins for reconstructions of changes in the global carbon cycle.

Until recently, fossiliferous Boreal outcrops with J–K boundary strata escaped the close attention of scientists mainly because of their inaccessibility. The Nordvik section in northern East Siberia was the first Boreal section where $\delta^{13}C$ and $\delta^{18}O$ curves were reconstructed for the J–K

* Corresponding author. Tel.: +7 383 3332306; fax: +7 383 3332301.
E-mail addresses: dzyubaos@ipgg.sbras.ru (O.S. Dzyuba), izokhop@gmail.com (O.P. Izokh), shuryginbn@ipgg.sbras.ru (B.N. Shurygin).

0031-0182/$ – see front matter © 2013 Elsevier B.V. All rights reserved.
http://dx.doi.org/10.1016/j.palaeo.2013.04.013

boundary interval; however, no significant excursions were found in the carbon or oxygen isotope records that could be used for further Boreal–Tethyan correlations around the J–K boundary (Žák et al., 2011). This lack of excursions was partially due to the high concentration of organic matter in the sediments, which could cause significant changes in the isotopic composition of carbonate material during diagenesis. As a result of the oxidation of organic matter and isotope exchange reactions between ^{12}C-enriched CO_2 and carbonate material, the $\delta^{13}C$ values of the carbonate material could be considerably reduced (Vinogradov, 2009).

Another Boreal section with a stratigraphically-complete sequence of sediments spanning the Volgian–Ryazanian boundary is located in the foothills of the Northern Urals on the Maurynya River in Western Siberia (Fig. 1). Well-preserved belemnite rostra that describe the J–K boundary interval in detail were collected from this section. This paper presents the results of the study of the variations of the carbon and oxygen isotopes in the rostra of this collection. Additional sampling of rostra was performed in the same stratigraphic interval in the Nordvik Peninsula.

1.2. Problems of Panboreal and Boreal–Tethyan correlations

In addition to Mesozoic ammonoid biostratigraphy, great importance has recently been placed on using integrated parallel (independent) zonal scales from different groups of fauna and flora to provide more detailed and reliable correlations (Zakharov et al., 1997; Hardenbol et al., 1998; Shurygin et al., 2000, 2011). Boreal zonal scales for the J–K boundary interval are based on ammonites (mainly Craspeditidae), belemnites (Cylindroteuthididae), bivalves (Buchiidae), microfossils and palynomorphs. High-latitude, mostly Eastern Siberian Boreal zonal successions have been accepted by some authors as a standard for Boreal basins in this interval (e.g., Baraboshkin, 2004; Shurygin et al., 2011; Bragin et al., 2013). These successions are widely distributed in northern Eurasia, northern North America and the Arctic islands, including Greenland, Spitsbergen and other locations (e.g., Surlyk et al., 1973; Saks, 1975; Callomon and Birkelund, 1982; Surlyk and Zakharov, 1982; Jeletzky, 1984; Shurygin et al., 2000, 2011; Nikitenko et al., 2008; Rogov and Zakharov, 2009; Rogov, 2010; Dzyuba, 2012, 2013). These scales work less successfully in low-latitude Boreal sections (northwestern Europe, the Russian Platform without the northern part, the Russian Far East, northeastern China, Western British Columbia and others) due to the provincialism observed to a variable degree in the fauna of these regions (e.g., Jeletzky, 1984; Zakharov, 1987, 2011; Casey et al., 1988; Sey and Kalacheva, 1999; Sha et al., 2003, 2006; Wimbledon, 2008; Rogov and Zakharov, 2009). Consequently, correlating the low-latitude Boreal J–K boundary successions with the Boreal standard is a complex task.

A fundamentally new scheme of subdividing the Ryazanian Stage of the Russian Platform based on ammonites is currently being developed (Mitta, 2007; Mitta and Sha, 2011). The main problem of this scheme, however, is the validity of the placement of the *Hectoroceras kochi* Zone to the base of the Ryazanian Stage before the *Riasanites rjasanensis* Zone (for a discussion see Bragin et al., 2013). The more traditional view on the ammonite zonation of the Ryazanian of the Russian Platform is adopted within this work (Fig. 2). For the upper

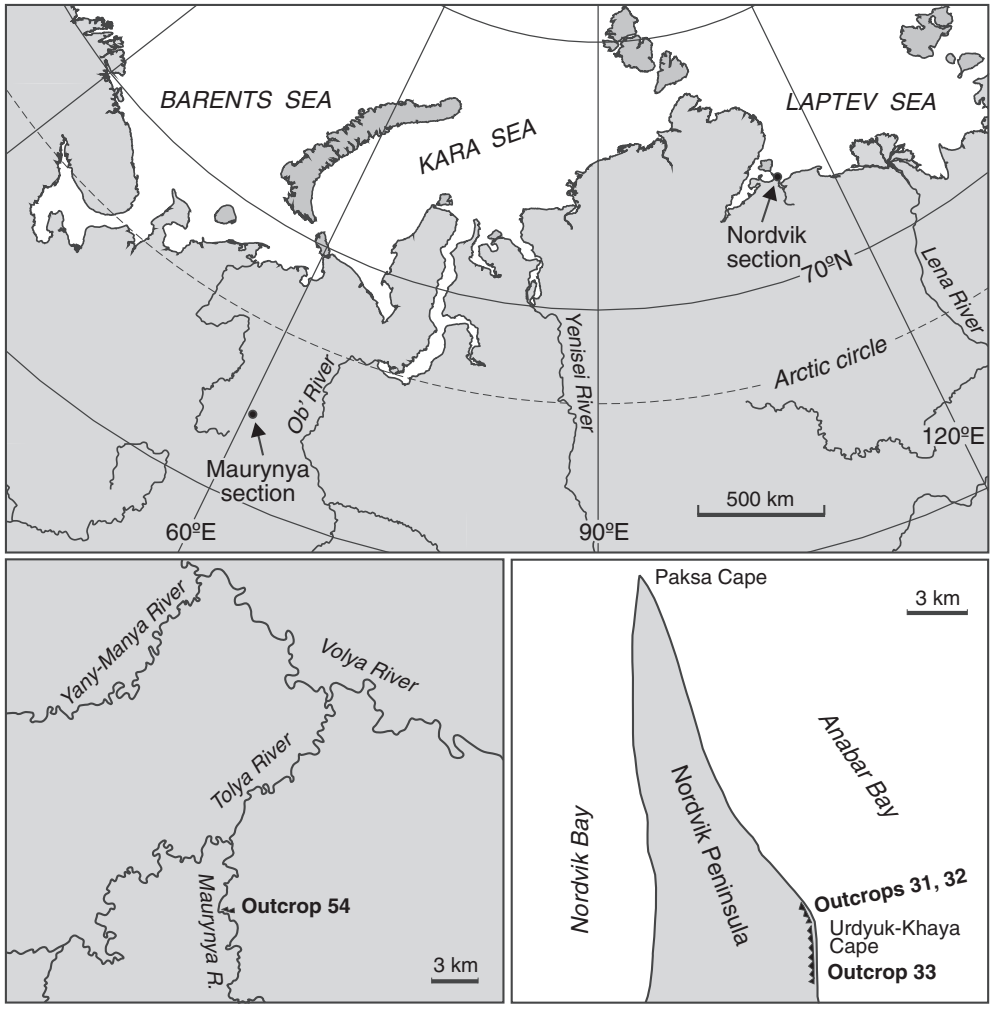

Fig. 1. The locations of the studied Maurynya and Nordvik sections in Siberia.

Volgian, a scheme proposed by Rogov and Zakharov (2009) is used, even though not all the stratigraphic units proposed by these authors can be considered as commonly used. Thus, according to Mitta (2010), the index species of the topmost beds of the Volgian Stage in the Russian Platform called the *Volgidiscus singularis* Kiselev, first identified by Kiselev (2003), is unrelated to *Volgidiscus*. Mitta considers the holotype of *V. singularis* as *Kachpurites mola* (Kiselev) and argues for a lower stratigraphic position of the beds with '*V. singularis*', at the base of the *Craspedites subditus* Zone of the upper Volgian.

The Boreal–Tethyan correlation of the J–K boundary interval is a stratigraphic problem that cannot be solved solely by using the biostratigraphic method. This problem is rooted in the fact that the latest Jurassic and earliest Cretaceous was a time of extreme differences between the Boreal and Tethyan marine biota. As a result, the Tithonian and Berriasian stages, which are between the Kimmeridgian and Valanginian stages, are assigned to the Tethyan scale, while the Volgian and Ryazanian stages are assigned to the Boreal scale. Significant progress in the correlation of the 'Boreal' and 'Tethyan' Berriasian has been made due to the discovery of Tethyan ammonites in the *Riasanites rjasanensis* Zone of the Russian Platform (Mitta, 2008, 2011). However, the J–K boundary intervals of the two realms have been compared more precisely using high resolution magnetostratigraphy (Houša et al., 2007; Bragin et al., 2013) than using biostratigraphy.

Non-palaeontological methods of correlation in general should play an important role in positioning the J–K boundary. The Global Stratotype Section and Point (GSSP) for the Berriasian, the basal stage of the Cretaceous, is currently under consideration by the Cretaceous International Subcommission of the IUGS; however, it is difficult to establish based on ammonites because of their ubiquitous provincialism and lack of reliable index taxa (Ogg et al., 1991; Remane, 1991; Wimbledon, 2008; Wimbledon et al., 2011; Zakharov, 2011). An integration of both palaeontological (nanno-, micro- and macrofossil stratigraphy) and non-palaeontological (magneto- and chemostratigraphy) methods can solve the problem of marker selection for the J–K boundary. In this paper, we demonstrate the possibility of using carbon-isotope stratigraphy to solve the J–K boundary interval problems.

1.3. Objectives

The main aims of our investigation are: (1) to construct a detailed carbon-isotope curve for the J–K boundary transition in Western Siberia; (2) to produce a more detailed carbon-isotope curve for the

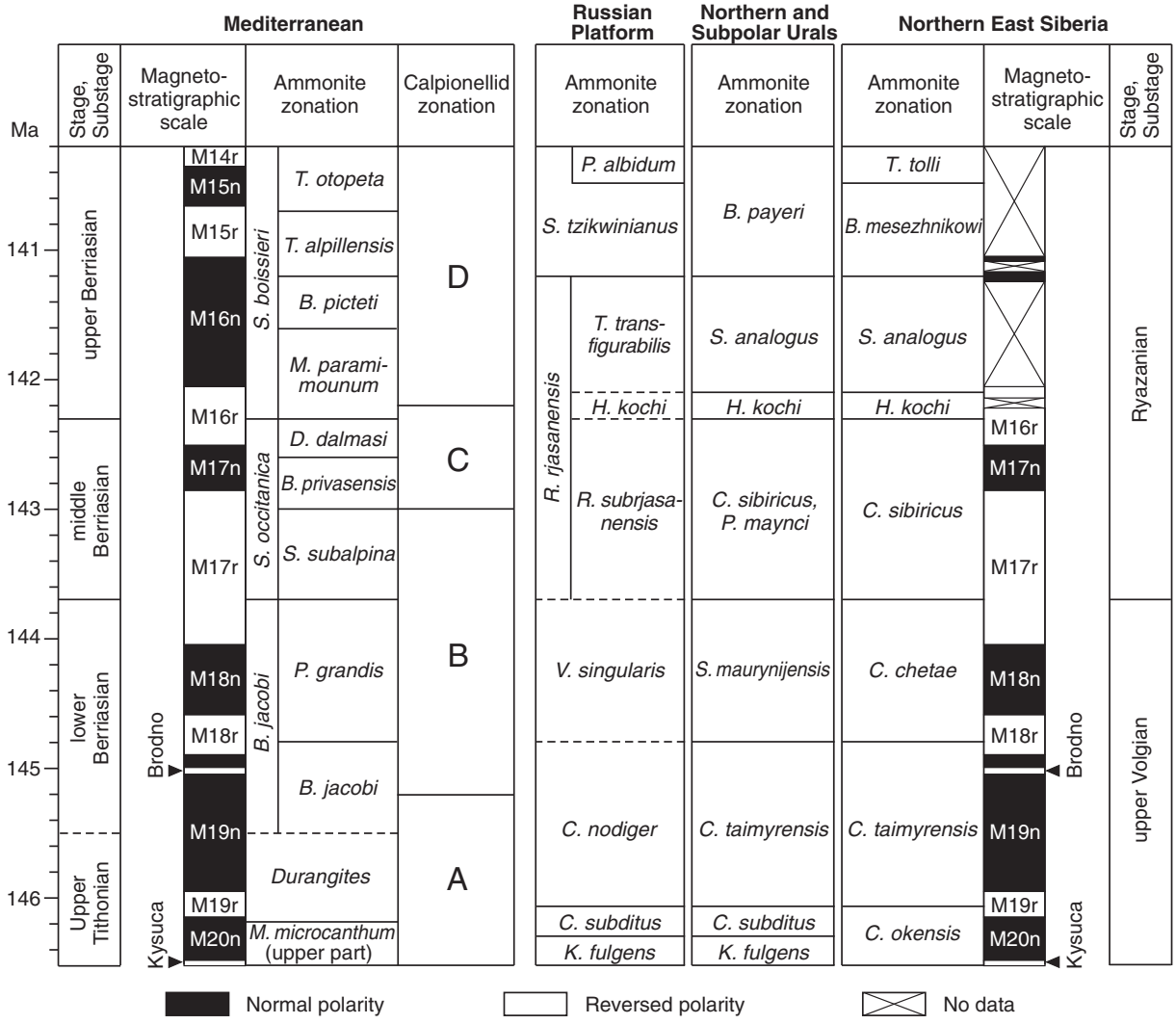

Fig. 2. Bio- and magnetostratigraphy across the J–K boundary in the Mediterranean (Gradstein et al., 2004; Hoedemaeker et al., 2003; Pruner et al., 2010), Russian Platform (Baraboshkin, 2004; Rogov and Zakharov, 2009), Northern and Subpolar Urals (Saks, 1975; Gurari, 2004) and northern East Siberia (Zakharov et al., 1997; Houša et al., 2007; Bragin et al., 2013). Correlations are based on Casey et al. (1988), Mesezhnikov (1989), Gradstein et al. (2012) and Rogov and Zakharov (2009) with corrections according to Bragin et al. (2013). The base of the Berriasian is placed at the base of the *Berriasella jacobi* ammonite Subzone, in accordance with the decision of 'Colloque sur la limite Jurassique–Crétacé' of 1973 (Flandrin et al., 1975) and Gradstein et al. (2004) time scale, and is marked with dashed line, because the exact position of this level with respect to magnetostratigraphic scale is not defined (Gradstein et al., 2012; Pruner et al., 2010; Wimbledon et al., in press).

J–K boundary transition in Eastern Siberia than currently exists; (3) to construct a composite carbon-isotope curve for the upper Volgian and Ryazanian in Boreal regions; and (4) to compare the carbon isotope records of the J–K boundary sections located in the Boreal and Tethyan areas.

2. Studied sections and materials

2.1. The Maurynya section

The Maurynya section is located approximately 125 km south of the West Siberian town of Saranpaul' (Fig. 1, 63°10′55.2″N, 60°16′0.02″E). The total thickness of the continuous upper Volgian and lowermost Ryazanian shallow marine sedimentary succession exposed along the right bank of the Maurynya River is 6 m. The section is extremely rich in fossils, including belemnites. The following cylindroteuthid belemnite zones and beds have been established in the section: the *Lagonibelus napaensis* Zone, *Simobelus compactus* beds, the *Cylindroteuthis knoxvillensis* Zone, and *Boreioteuthis explorata* beds (Dzyuba, 2013). The uppermost 3.5 m of the section is well characterised by ammonites of the *Craspedites taimyrensis* Zone to the lowermost part of the *Hectoroceras kochi* Zone (Alifirov et al., 2008). The basal upper Volgian part of the section comprises bluish-grey sandstones, with minor siltstone and silty mudstone beds, whereas the uppermost Volgian–lowermost Ryazanian portion is dominated by greenish-grey glauconitic sandstones with occasional concretions. The fossil cephalopods and the presence of glauconite in the section indicate a marine sedimentary setting in the Maurynya River region during the time of the Jurassic–Cretaceous transition. According to Smith et al. (1994), this basin was situated at the palaeolatitude of ~60°N.

2.2. The Nordvik section

The Nordvik section is located on the Nordvik Peninsula (northern East Siberia) between Nordvik Bay and Anabar Bay. The J–K boundary strata are well exposed in the Urdyuk–Khaya Cape area (Fig. 1, 73°52′ 36″N, 113°08′33″E). Two individual outcrops (32 and 33) along the coast of Anabar Bay expose a continuous sedimentary succession across the J–K boundary, whereas outcrop 31 exposes middle Ryazanian strata (Zakharov et al., 1983). The interval from the middle Volgian *Epivirgatites variabilis* ammonite Zone to the Ryazanian *Hectoroceras kochi* ammonite Zone of the composite Nordvik section, which is approximately 26 m thick, was studied. The section is also well-characterised by cylindroteuthid belemnites (Dzyuba, 2012), bivalves (Zakharov et al., 1983; Zakharov and Rogov, 2008), foraminifers and dinocysts (Nikitenko et al., 2008). Moreover, all of magnetozones M20n to M17n, including two important subzones (M20n.1r, the Kysuca Subzone, and M19n.1r, the Brodno Subzone), and part of magnetozone M16r were established around the J–K boundary interval in this section (Houša et al., 2007; Bragin et al., 2013). The studied section is lithologically homogenous and comprises dark grey claystones with occasional calcareous nodular horizons. The sedimentary environment is interpreted as a distal offshore marine setting with water depths of 150–200 m and deeper (Zakharov and Judovnyi, 1974), which explains the scarcity of belemnite rostra and therefore makes it difficult to study the boundary interval in detail. According to Smith et al. (1994), in the J–K time this basin was located at the palaeolatitude of ~75°N. The reducing conditions in the sediments during diagenesis led to the formation of diagenetic pyrite through the reduction of dissolved sulphate in the pore water (Žák et al., 2011).

2.3. Belemnites

Sixty-one Volgian–Ryazanian cylindroteuthid belemnites were collected from both localities. In the Maurynya section, the belemnites were collected from 25 levels; in the Nordvik section, they were collected from 36 levels. The belemnites sampled from the Maurynya section are composed of translucent light-honey-coloured calcite, and the majority of the belemnites from the Nordvik section are composed of translucent dark-honey-coloured calcite. In addition, the rostra at some stratigraphic levels in the Nordvik section are either encrusted by pyrite grains or contain pyrite within the growth layers and, to a lesser degree, along the central line, as was earlier observed by Žák et al. (2011).

The sampled belemnites belong to the following genera: *Arctoteuthis* (46%), *Boreioteuthis* (7%), *Cylindroteuthis* (7%), *Lagonibelus* (21%), *Pachyteuthis* (3%) and *Simobelus* (5%). With the exception of *Simobelus*, these belemnites were presumably active to moderately active epipelagic swimmers based on their stream-lined bodies, fins and the epipelagic depths (<200 m) where they dwelled (Dzyuba, 2013; Zakharov et al., in press). *Simobelus*, which is characterised by a short robust rostrum, was a lightly active (? nektobenthic) animal that preferred shallow near-shore water (Zakharov et al., in press). Gustomesov (1976) considered *Boreioteuthis*-like cylindroteuthids that had a moderately elongate ventrally flattened rostrum with a long and wide ventral groove to be bottom-dwelling organisms; however, Mutterlose et al. (2010) argued that members of the Hauterivian–Barremian genus *Aulacoteuthis* (convergent with the genus *Boreioteuthis*) were active swimmers. Recently, belemnite palaeoecology has been an active topic of discussion. On the one hand, the observed similarities in the oxygen isotope compositions of belemnites, brachiopods and bivalves indicate a nektobenthic habit for belemnites (e.g., Anderson et al., 1994; Wierzbowski, 2002; Wierzbowski and Joachimski, 2007; Wierzbowski and Rogov, 2011). On the other hand, the occurrence of belemnites in black shales deposited under anoxic bottom water conditions (e.g., Mutterlose, 1983; Seilacher et al., 1985; Oschmann et al., 1999) argues for a nektonic habit for at least some belemnite genera (Rexfort and Mutterlose, 2009).

Because approximately 11% of the cylindroteuthid belemnites in our collection are not completely preserved, specific identification and generic identification are difficult. All of the identified species are unknown from the Boreal-Atlantic Realm and from Tethys. Most of the identified species (*Arctoteuthis repentina*, *Boreioteuthis explorata*, *Cylindroteuthis jacutica*, *Lagonibelus gustomesovi*, *Lagonibelus sibiricus*, *Pachyteuthis acuta*, and *Simobelus compactus*) inhabited the Boreal Arctic Sea, whereas others (*Arctoteuthis porrectiformis*, *Arctoteuthis tehamaensis*, *Cylindroteuthis knoxvillensis*, and *Lagonibelus napaensis*) could have migrated over long distances through the epicontinental seaway between Siberia and Northern California (Dzyuba, 2012, 2013). Thus, the obtained oxygen isotope data for some of the belemnite species can depend on a non-endemic way of life.

3. Methods

The carbon and oxygen isotope variations in the belemnite rostra mirror that of ancient seawater and can be preserved over time (Sælen et al., 1996; Price and Sellwood, 1997; Niebuhr and Joachimski, 2002; Price and Mutterlose, 2004; Rosales et al., 2004; Zakharov et al., 2005; Wierzbowski and Joachimski, 2007; Wierzbowski and Rogov, 2011). Based on recent observations (e.g., McArthur et al., 2004; Wierzbowski and Rogov, 2011; Zakharov et al., in press), differences in metabolic fractionation or ecology may cause a discrepancy in isotope values for different belemnite families or genera, but these factors do not strongly affect the isotope composition of belemnite calcite; as Jenkyns et al. (2002) already stated, reproducible long-term oxygen isotope trends may be recognised, and stratigraphically-correlatable carbon isotope signals may be definable.

However, the $\delta^{13}C$ and $\delta^{18}O$ values and the chemical composition of the carbonates can be modified as a result of post-depositional diagenetic alteration of the carbonate material in the belemnite rostra. Different methods were applied to identify samples with diagenetically-altered C- and O-isotope values. One method is the investigation of polished

belemnite chips using cathodoluminescence, where diagenetically-altered parts of belemnites are characterised by luminescence. Intense cathodoluminescence of carbonate material is due to high concentrations of Mn^{2+} and Fe^{2+} in $CaCO_3$ (Machel, 1985) that usually are the result of the diagenetical alteration processes (Veizer, 1983). Another method uses geochemical criteria to distinguish altered from non-altered samples via the Fe, Mn and Sr contents of carbonates. Low Sr concentrations and high Fe and Mn concentrations in the meteoric waters and diagenetic fluids lead to a decrease in the Sr contents and an increase in the Fe and Mn contents of shell carbonates during post-depositional alteration (Brand and Veiser, 1980). Different authors have used different concentrations of these elements as limiting criteria (e.g., Anderson et al., 1994; Ditchfield, 1997; Price and Mutterlose, 2004). Nevertheless, the ultimate factor in identifying diagenetically-altered samples is the correlation between the isotopic compositions of carbon and oxygen and the Fe and Mn contents.

The state of preservation of the studied belemnite rostra material was determined using the Centaurus Cathodoluminescence Detector in a LEO1430VP scanning electron microscope (SEM). The altered exterior and central parts of the belemnites (Fig. 3a, b) were removed, and the remaining parts of the samples were powdered in an agate mortar. To determine the Ca, Mg, Fe, Mn and Sr contents, 100 mg samples were dissolved in 1N HCl. Careful dissolution in an unsaturated acid solution avoids contamination by the components of siliciclastic material. The siliciclastic content in the samples reaches 3.8% and is 0.6% on average. The Ca, Mg, Fe, Mn and Sr contents in the soluble part of the carbonates were determined on an SP9 PI UNICAM atomic-absorption spectrometer. The determination error was less than 10%.

The isotopic composition of the carbon dioxide was measured by mass spectrometry in a continuous helium flow. A mass-spectrometric complex, including a Finnigan MAT-253 mass spectrometer and a Gas Bench II sample preparation line, were used to analyse the isotopic compositions of oxygen and carbon in the carbonate. For the measurements, we used pure CO_2 produced by the decomposition of carbonate powder in orthophosphoric acid for 2 h at 60 °C. The accuracy of the carbon and oxygen determination in the carbonates (0.1‰ for both $\delta^{13}C$ and $\delta^{18}O$) was controlled by analysis of international (NBS19 $\delta^{13}C = +1.9‰$, $\delta^{18}O = -2.2‰$) standard samples.

All of the analyses were carried out at the Analytical Center of the Sobolev Institute of Geology and Mineralogy, Novosibirsk.

4. Results

4.1. Post-depositional changes

Examination of polished plates from the belemnite rostra collections with cathodoluminescence radiation revealed that the majority of the selected material had no significant signs of post-depositional changes. Only a few samples were characterised by the luminescence of exterior or apical parts (Fig. 3a, b) or a significant part of the rostrum (Fig. 3c).

All of the studied belemnite rostra were characterised by high concentrations of strontium (900–1762 ppm in the Nordvik section, and 1022–1443 ppm in the Maurynya section), suggesting a high degree of preservation of the belemnite carbonate material (Rosales et al., 2001, 2004). A small number of samples in the Nordvik section are characterised by high concentrations of iron and manganese (Table 1). The highest concentrations of Fe (up to 3624 ppm) and Mn (up to 615 ppm) are typical of the samples characterised by luminescence and re-crystallisation of the carbonate material.

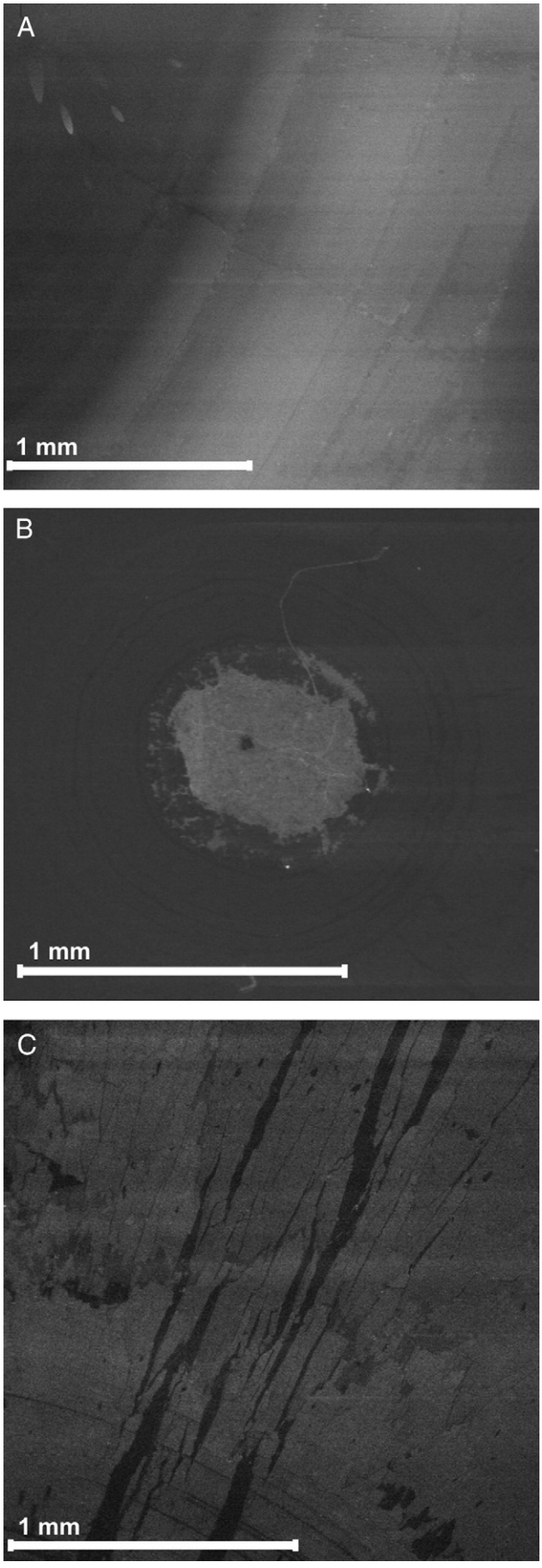

Fig. 3. Cathodoluminescence photomicrographs of belemnite rostra. (A) Luminescent external growth lines of the rostrum. Sample MR54.1-20. (B) Luminescent apical line area of the rostrum. Sample NP32.5-20. (C) Strongly luminescent rostrum. Sample NP32.7-100.

Table 1
Stable isotope data (belemnite rostra, in ‰ vs. V-PDB) and chemical composition of samples (in ppm) from the Maurynya and Nordvik sections. Bold font denotes diagenetically-altered samples (Mn content >100 ppm; Fe content >150 ppm) that were not included in the diagrams and were rejected from subsequent analyses.

Sample ID	Location	Position	Ammonite biozone	Taxonomy	$\delta^{13}C$	$\delta^{18}O$	Mn	Fe	Sr	Mg	Ca
		m			(‰)		(ppm)				
MR54.1-10	Maurynya River	0.10		*Lagonibelus* cf. *napaensis*	−0.5	−0.6	30	100	1020	749	393,000
MR54.1-20	Maurynya River	0.20		*Arctoteuthis* cf. *porrectiformis*	1	−0.6	29	8	1080	766	379,000
MR54.2-00	Maurynya River	0.50		*Boreioteuthis* cf. *explorata*	1.4	−0.2	11	57	1210	877	389,000
MR54.3-20	Maurynya River	1.05		*Boreioteuthis explorata*	0.5	−0.8	2	5	1280	981	391,000
MR54.3-105	Maurynya River	1.90		*Boreioteuthis* cf. *explorata*	0.4	−0.2	4	5	1140	880	380,000
MR54.4-10	Maurynya River	2.30		*Boreioteuthis* cf. *explorata*	0.2	−2.0	9	17	1280	918	367,000
MR54.5-00	Maurynya River	2.45		*Simobelus* cf. *compactus*	0.3	−0.2	2	5	1290	711	373,000
MR54.5-20	Maurynya River	2.65		*Simobelus* cf. *compactus*	0.8	−1.4	17	4	1320	613	376,000
MR54.5-30	Maurynya River	2.75		*Simobelus* cf. *compactus*	1.6	−0.9	4	2	1440	645	372,000
MR54.5-45	Maurynya River	2.90	*taimyrensis*	*Pachyteuthis* cf. *acuta*	0.7	−1.1	16	4	1240	673	369,000
MR54.5-50	Maurynya River	2.95	*taimyrensis*	*Lagonibelus* cf. *napaensis*	0.8	−1.3	4	20	1120	1270	385,000
MR54.5-55	Maurynya River	3.00	*taimyrensis*	*Lagonibelus* cf. *napaensis*	0.9	−1.1	17	14	1270	742	361,000
MR54.5-60	Maurynya River	3.05	*taimyrensis*	*Lagonibelus* cf. *napaensis*	0.8	−0.9	7	19	1370	710	354,000
MR54.5-70	Maurynya River	3.15	*taimyrensis*	*Lagonibelus* cf. *napaensis*	0.6	−0.7	5	6	1350	586	362,000
MR54.5-85	Maurynya River	3.30	*maurynijensis*	*Lagonibelus* cf. *napaensis*	−0.3	−1.6	3	31	1100	914	355,000
MR54.5-95	Maurynya River	3.40	*maurynijensis*	indet.	0	−1.2	8	5	1120	1030	360,000
MR54.6-00	Maurynya River	3.45	*maurynijensis*	*Lagonibelus* cf. *gustomesovi*	−0.5	−2.0	6	6	1150	1340	353,000
MR54.6-25	Maurynya River	3.70	*maurynijensis*	*Lagonibelus* cf. *napaensis*	−0.4	−1.3	6	5	1160	661	381,000
MR54.6-30	Maurynya River	3.75	*maurynijensis*	*Lagonibelus* cf. *gustomesovi*	−0.1	−1.7	8	15	1090	1030	381,000
MR54.6-50	Maurynya River	3.95	*maurynijensis*	*Pachyteuthis sp.*	0	−1.2	12	9	1300	837	394,000
MR54.6-85	Maurynya River	4.30	*maurynijensis*	*Lagonibelus gustomesovi*	0	−0.9	9	5	1340	835	382,000
MR54.7-05	Maurynya River	4.60	*sibiricus*	*Lagonibelus* cf. *gustomesovi*	−0.1	−0.8	3	13	1240	914	383,000
MR54.7-25	Maurynya River	4.80	*sibiricus*	indet.	−0.1	−1.6	5	5	1340	978	378,000
MR54.8-05	Maurynya River	4.90	*sibiricus*	*Arctoteuthis* cf. *repentina*	0.3	−1.6	6	65	1290	709	388,000
MR54.9-10	Maurynya River	5.55	*kochi*	*Arctoteuthis repentina*	−0.4	−1.1	4	5	1370	1200	385,000
NP33.8-20	Nordvik Peninsula	0.20	*variabilis*	*Cylindroteuthis jacutica*	0.2	0.8	26	103	950	1540	369,000
NP32.4-55	Nordvik Peninsula	4.70	*exoticus*	indet.	0.9	−1.5	22	108	1040	853	388,000
NP32.5-20	Nordvik Peninsula	6.55	*okensis*	*Lagonibelus sibiricus*	0	**−1.0**	**160**	**1230**	**990**	**950**	**379,000**
NP32.6-80	Nordvik Peninsula	8.10	*okensis*	*Arctoteuthis* cf. *porrectiformis*	**0.3**	**−1.4**	**97**	**1553**	**969**	**1050**	**377,000**
NP32.7-100	Nordvik Peninsula	9.15	*okensis*	*Arctoteuthis* cf. *porrectiformis*	**0.5**	**−0.7**	**257**	**3624**	**900**	**924**	**374,000**
NP32.8-105	Nordvik Peninsula	10.25	*taimyrensis*	*Lagonibelus* cf. *gustomesovi*	0.1	0.8	16	15	1100	692	372,000
NP32.9-15	Nordvik Peninsula	10.85	*taimyrensis*	*Arctoteuthis* cf. *porrectiformis*	0.1	−0.5	23	36	947	1240	370,000
NP32.9-40	Nordvik Peninsula	11.10	*taimyrensis*	*Arctoteuthis* cf. *porrectiformis*	0	0.6	22	38	1250	770	363,000
NP32.9-170	Nordvik Peninsula	12.40	*taimyrensis*	*Arctoteuthis* cf. *tehamaensis*	0.2	0.1	12	24	1080	805	376,000
NP32.9-230	Nordvik Peninsula	13.00	*taimyrensis*	*Arctoteuthis* cf. *tehamaensis*	**0.3**	**−1.3**	**93**	**654**	**967**	**1790**	**367,000**
NP32.9-240	Nordvik Peninsula	13.10	*taimyrensis*	*Arctoteuthis* cf. *porrectiformis*	0.9	−0.2	22	53	1130	840	380,000
NP32.10-10	Nordvik Peninsula	13.40	*chetae*	*Arctoteuthis* cf. *porrectiformis*	0.2	−0.9	19	27	980	1070	381,000
NP32.10-65	Nordvik Peninsula	13.95	*chetae*	*Arctoteuthis* cf. *porrectiformis*	−0.1	−0.6	12	16	1070	1120	383,000
NP32.10-102	Nordvik Peninsula	14.32	*chetae*	*Arctoteuthis tehamaensis*	−0.9	−0.6	35	33	1050	1040	367,000
NP32.12-35	Nordvik Peninsula	14.90	*sibiricus*	*Arctoteuthis* cf. *tehamaensis*	0.8	0.0	19	30	1260	920	359,000
NP32.12-100	Nordvik Peninsula	15.55	*sibiricus*	*Arctoteuthis tehamaensis*	0.7	−1.5	17	20	1010	832	373,000
NP32.13-30	Nordvik Peninsula	15.95	*sibiricus*	*Arctoteuthis tehamaensis*	0.3	−1.7	70	62	1090	1050	375,000
NP32.13-45	Nordvik Peninsula	16.10	*sibiricus*	indet.	0.1	−0.4	68	71	1410	772	376,000
NP32.13-55	Nordvik Peninsula	16.20	*sibiricus*	*Arctoteuthis sp.*	0.1	0.4	45	21	1220	1040	378,000
NP32.13-70	Nordvik Peninsula	16.35	*sibiricus*	*Arctoteuthis sp.*	**−0.2**	**−1.2**	**87**	**210**	**1030**	**1160**	**378,000**
NP32.14-10	Nordvik Peninsula	16.50	*sibiricus*	*Cylindroteuthis knoxvillensis*	−0.2	−0.5	51	73	1270	778	381,000
NP32.14-35	Nordvik Peninsula	16.75	*sibiricus*	*Arctoteuthis* cf. *porrectiformis*	1.2	−0.3	56	75	1090	729	377,000
NP32.14-40	Nordvik Peninsula	16.80	*sibiricus*	*Arctoteuthis* cf. *repentina*	0.6	−0.4	30	22	1140	1390	372,000
NP32.14-55	Nordvik Peninsula	16.95	*sibiricus*	*Arctoteuthis* cf. *repentina*	0.1	−0.3	74	78	1140	1690	368,000
NP32.14-60	Nordvik Peninsula	17.00	*sibiricus*	indet.	**−2.6**	**−2.2**	**615**	**3268**	**1760**	**1530**	**388,000**
NP32.14-65	Nordvik Peninsula	17.05	*sibiricus*	*Arctoteuthis* cf. *repentina*	0.4	−0.3	22	17	1120	851	373,000
NP32.15-20	Nordvik Peninsula	17.30	*sibiricus*	*Cylindroteuthis cf. knoxvillensis*	**0.5**	**0**	**125**	**377**	**1580**	**913**	**375,000**
NP32.15-80	Nordvik Peninsula	17.90	*sibiricus*	*Arctoteuthis* cf. *tehamaensis*	**−1.3**	**0.7**	**110**	**123**	**1420**	**907**	**375,000**
NP32.15-105	Nordvik Peninsula	18.15	*sibiricus*	indet.	**−1.1**	**−3.2**	**377**	**1306**	**1580**	**1070**	**381,000**
NP32.16-70	Nordvik Peninsula	18.90	*sibiricus*	*Cylindroteuthis* cf. *knoxvillensis*	0	0.5	17	9	1090	1070	391,000
NP32.16-110	Nordvik Peninsula	19.30	*sibiricus*	*Arctoteuthis* cf. *tehamaensis*	−0.3	0.5	78	102	1040	1030	388,000
NP32.16-135	Nordvik Peninsula	19.55	*sibiricus*	indet.	**0.6**	**−1.3**	**79**	**177**	**1050**	**825**	**391,000**
NP32.16-150	Nordvik Peninsula	19.70	*sibiricus*	*Arctoteuthis* cf. *porrectiformis*	1.5	−0.4	96	77	1010	912	394,000
NP32.18-55	Nordvik Peninsula	21.15	*kochi*	*Arctoteuthis* cf. *porrectiformis*	**0.9**	**−1**	**174**	**73**	**1180**	**870**	**380,000**
NP31.3-10	Nordvik Peninsula	23.50	*kochi*	*Arctoteuthis* cf. *porrectiformis*	1.4	1.9	53	72	1060	593	412,000
NP31.3-180	Nordvik Peninsula	25.20	*kochi*	*Arctoteuthis* cf. *porrectiformis*	1	−1.1	23	17	1390	718	378,000

An analysis of binary diagrams showed a relationship between the changes in the Fe and Mn concentrations in a small number of the samples with high concentrations of these elements (Fig. 4a). In addition, the lowest $\delta^{18}O$ values corresponded with higher concentrations of Mn and/or Fe (Fig. 4b, c). A similar correlation was observed for some of the samples on $\delta^{13}C$–Mn and $\delta^{13}C$–Fe binary diagrams (Fig. 4d, e), suggesting post-depositional alteration of the carbonate material of the belemnite rostra at some levels of the Nordvik section. As a result, displacements of the primary $\delta^{18}O$ and $\delta^{13}C$ values are observed. These samples were excluded from further consideration. The Mn and Fe concentrations in the other samples were less than 100 ppm and 150 ppm, respectively, and did not exceed the threshold concentrations of these elements that are accepted by many authors as indicators of high degrees of carbonate material preservation in belemnite rostra (e.g., Price and Mutterlose, 2004; Nunn et al., 2010).

4.2. Oxygen and carbon isotope variations

The Maurynya and Nordvik sections are characterised by similar trends of oxygen isotope variations within the same stratigraphic interval; the only difference is that the average $\delta^{18}O$ values in the Maurynya section are lower than those in the Nordvik section. The $\delta^{18}O$ values in the Maurynya section vary from −2.0 to −0.2‰ with an average of −1.1‰ (Table 1, Fig. 5) and are characterised by a generally decreasing upward trend to the upper part of the section. In the upper Volgian–lowermost Ryazanian (*Craspedites okensis–Chetaites sibiricus* ammonite zones) of the Nordvik section, the mean $\delta^{18}O$ value is −0.3‰, and the values range from −1.7 to 0.8‰ (Table 1, Fig. 6). The $\delta^{18}O$ values show an overall trend towards negative values from the middle Volgian to the base of the Ryazanian. The minimum $\delta^{18}O$ value (−1.7‰) is observed in the lower part of the *C. sibiricus* Zone within the lowermost part of magnetozone M17n. The values increase upward in the *C. sibiricus* Zone and vary insignificantly from −0.5‰ to +0.5‰. In the uppermost part of the section, which corresponds to the middle part of the *H. kochi* ammonite Zone, the $\delta^{18}O$ values increase up to 1.9‰ and then decrease to −1.1‰ (Fig. 6).

The $\delta^{13}C$ values in the Maurynya section range from −0.5 to +1.6‰ with a general decreasing upwards trend and include two large positive excursions (Fig. 5). The first excursion is defined in the lower part of the section, near the base of the *Boreioteuthis explorata* belemnite beds, where the $\delta^{13}C$ values increase from −0.5‰ to 1.4‰ and then decrease to almost 0‰. The second excursion is in the top part of the *Craspedites taimyrensis* ammonite Zone and is characterised by an increase in $\delta^{13}C$ values up to 1.6‰ and a subsequent decrease to −0.5‰ in the basal part of the *Subcraspedites maurynijensis* ammonite beds. In addition, a small positive shift is recognised in the *Chetaites sibiricus* ammonite Zone.

A $\delta^{13}C$ curve was reconstructed for the J–K boundary interval of the Nordvik section (Fig. 6). The curve essentially expands the curve that was first reconstructed by Žák et al. (2011) for the Middle Oxfordian–lowermost Ryazanian (*Cardioceras densiplicatum–Chetaites sibiricus* ammonite zones), which is characterised by lower data density at some levels. For example, the $\delta^{13}C$ curve for the *Craspedites taimyrensis–Chetaites chetae* zonal interval of Žák et al. (2011) consisted of only three points and contained no significant excursions. The curve based on the new data characterises the *C. taimyrensis–Hectoroceras kochi* ammonite zones of the Nordvik section and has its maximum data density in the *C. taimyrensis–C. sibiricus* zonal interval.

The $\delta^{13}C$ values in the studied interval of the Nordvik section vary from −0.9 to +1.5‰. In the top part of the *Craspedites taimyrensis* Zone, the $\delta^{13}C$ values increase from +0.2 (near the Brodno (M19n-1r) Subzone) to +0.9‰ (magnetozone M18r) and subsequently decrease to +0.2‰ at the base of the *Chetaites chetae* Zone and to −0.9‰ near its top (at the boundary between magnetozones M18n and M17r). The *Chetaites sibiricus* Zone is characterised by a gradual decrease of $\delta^{13}C$ values and includes two positive shifts in the middle and upper parts of the zone in which the $\delta^{13}C$ values increase from background values of 0–0.5‰ to 1.2‰ and 1.5‰, respectively (see Fig. 6). The middle part of the *Hectoroceras kochi* Zone is also characterised by high $\delta^{13}C$ values that vary between 1 and 1.4‰ (Fig. 6).

A comparison of the reconstructed $\delta^{13}C$ curve with the data from (Žák et al., 2011) with application of the geochemical criteria accepted during this study shows that the differences between samples of the same age did not exceed 0.2‰. Moreover, both sets of data show the same trends of $\delta^{13}C$ changes.

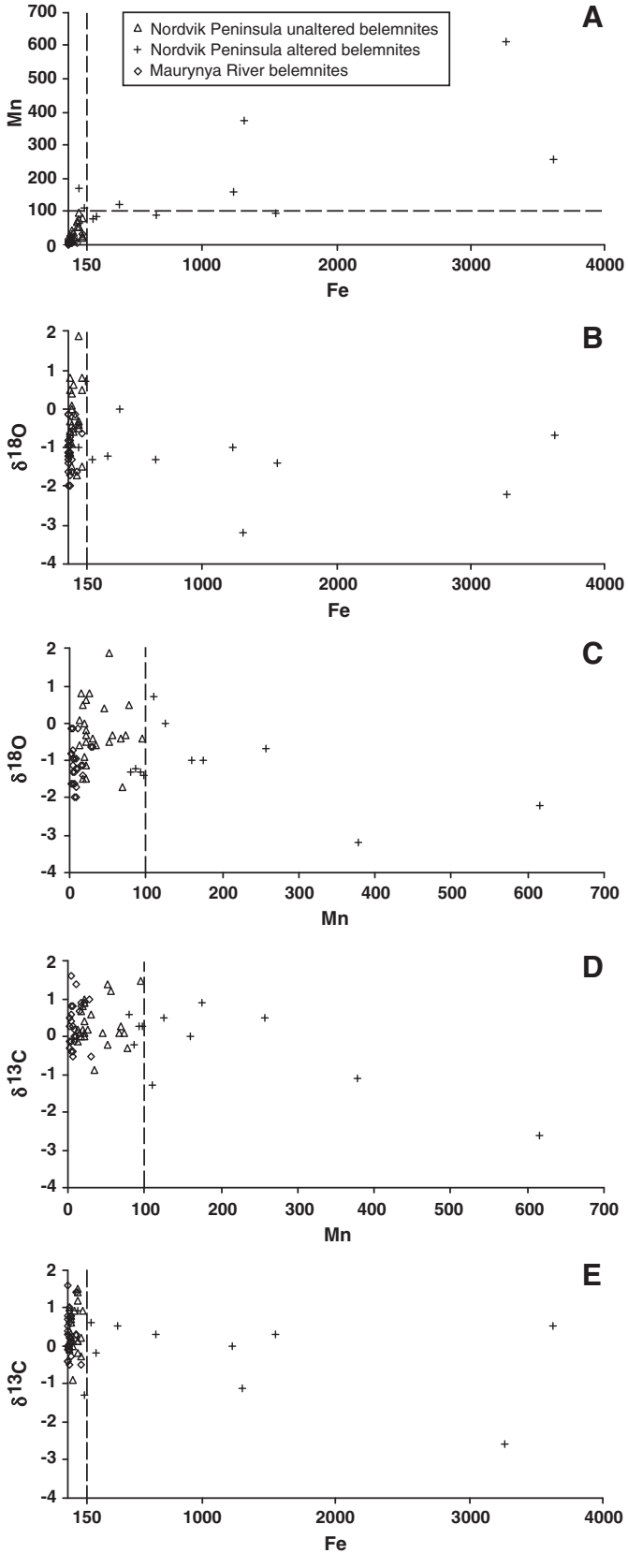

Fig. 4. (A) Fe versus Mn values. A correlation between the Fe and Mn values is observed in altered belemnite samples with high concentrations of these elements. (B) Fe versus $\delta^{18}O$ values. No correlation between the Fe and $\delta^{18}O$ values is observed in the diagenetically-unaltered belemnite rostra. (C) Mn versus $\delta^{18}O$ values. No correlation between the Mn and $\delta^{18}O$ values is observed in the diagenetically-unaltered belemnite rostra. (D) Mn versus $\delta^{13}C$ values. No correlation between the Mn and $\delta^{13}C$ values is observed in the diagenetically-unaltered belemnite rostra. (E) Fe versus $\delta^{13}C$ values. No correlation between the Fe and $\delta^{13}C$ values is observed in the diagenetically-unaltered belemnite rostra.

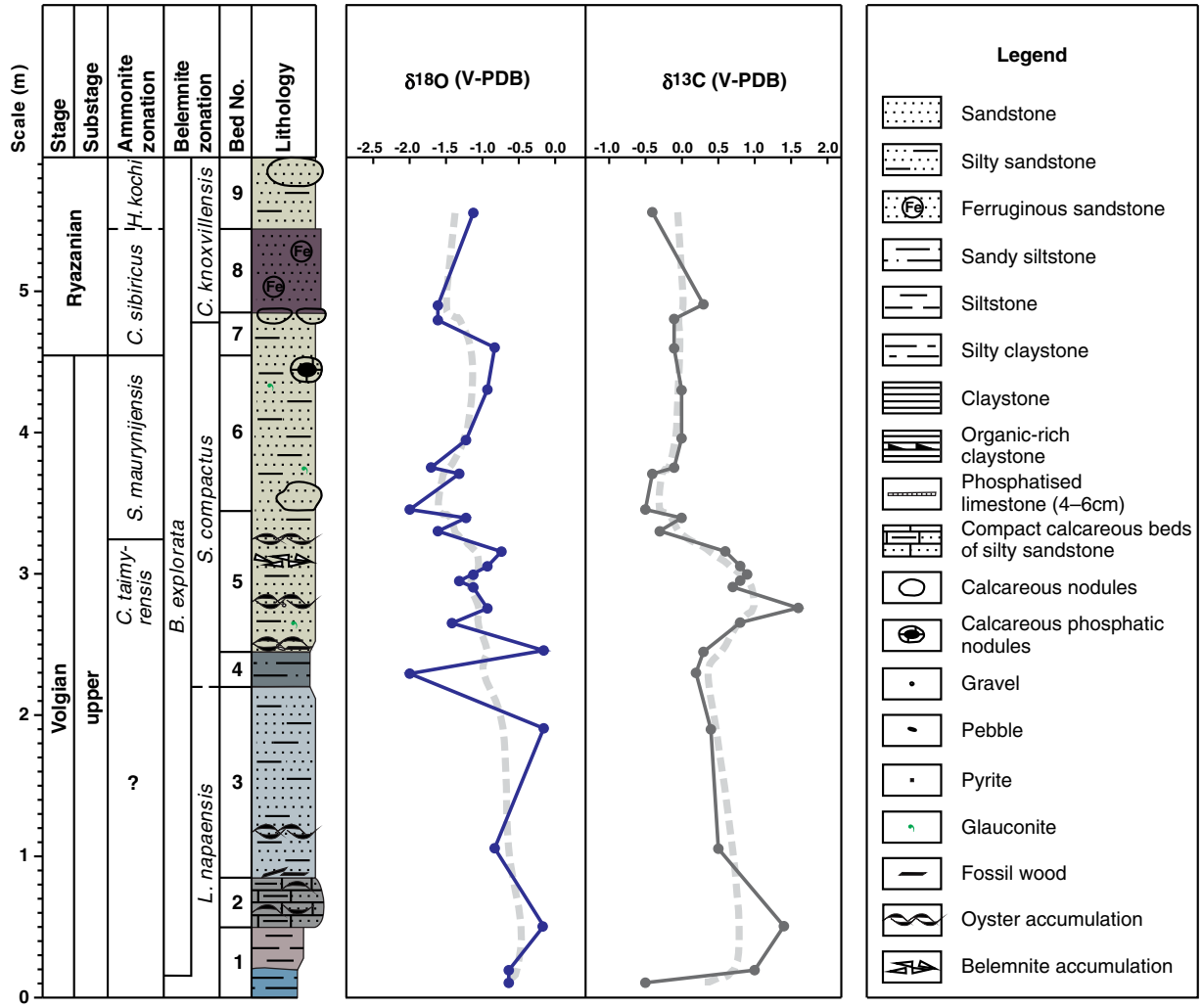

Fig. 5. Stable isotope signals at the Maurynya section (eastern slope of the Northern Urals, Western Siberia). Data are summarised using a 5-point moving average. Biostratigraphy and lithology are after Alifirov et al. (2008) and Dzyuba (2013).

5. Discussion

5.1. Palaeoenvironmental background

A comparison of the $\delta^{18}O$ curves obtained for the Maurynya and Nordvik sections showed an agreement between the general trends in the oxygen isotopic composition. The differences in $\delta^{18}O$ values in these sections are most likely due to the difference of water temperature in the marine basins, which is corroborated by the northern palaeogeographic position of the Nordvik section in comparison with the Maurynya section (Fig. 7). The negative trend in the $\delta^{18}O$ curve established for the Maurynya section was previously recorded in the Russian Platform (Price and Rogov, 2009) and Nordvik Peninsula (Žák et al., 2011) sections. The same trend was noted for the oxygen isotope variations obtained from Upper Tithonian–lower Berriasian bulk carbonates in Deep Sea Drilling Project Hole 534A in the central Atlantic Ocean (Tremolada et al., 2006). This trend is expressed less prominently in the Puerto Escaño section of southern Spain (Žák et al., 2011). This negative $\delta^{18}O$ trend is associated with a gradual warming of the climate from the Middle Oxfordian to the earliest Ryazanian (Abbink et al., 2001; Price and Rogov, 2009; Žák et al., 2011; Zakharov et al., in press). According to Dera et al. (2011), the $\delta^{18}O$ decrease during the Late Jurassic approximately corresponds to a period of prolonged and intensive magmatism in the northeast Asian igneous provinces (Wang et al., 2006) that could have caused high pCO_2 levels, which in turn could have maintained warmer climatic conditions.

The belemnite data show a trend towards heavier values of $\delta^{18}O$ (positive trend) only at the top of studied section across the *Chetaites sibiricus–Hectoroceras kochi* ammonite zonal boundary (Fig. 6). This trend coincides with the initiation of a climate cooling supposed for the earliest Cretaceous (e.g., Podlaha et al., 1998; Mutterlose and Kessels, 2000; Weissert and Erba, 2004). According to Abbink et al. (2001), the climatic shift in the North Sea region represented by a change from warm and arid to slightly cooler and humid conditions occurred in the *H. kochi* Zone. In Dorset (southern U.K.), the Durlston Bay and Lulworth Cove sections provide evidence of a climatic shift from semi-arid phase to more humid phase in the middle–late Berriasian (Schnyder et al., 2006, 2009). The reconstructed oxygen-isotope curves for the Maurynya and Nordvik sections show a correlation of the main $\delta^{18}O$ variations with the shift in climate from warm in the late Volgian to cooler in the middle–late Ryazanian, which was recognised in the Yatriya River (Western Siberia) successions (Price and Mutterlose, 2004). These earliest Cretaceous palaeoclimatic changes coincided with the decrease of atmospheric CO_2 levels established by Huang et al. (2012) from the early–middle Berriasian to the early Valanginian.

Global warming during the Late Jurassic was apparently favourable for life on Earth, which is observed in the increased diversity of marine fauna during this time (e.g., Newman, 2001). Although the J–K boundary

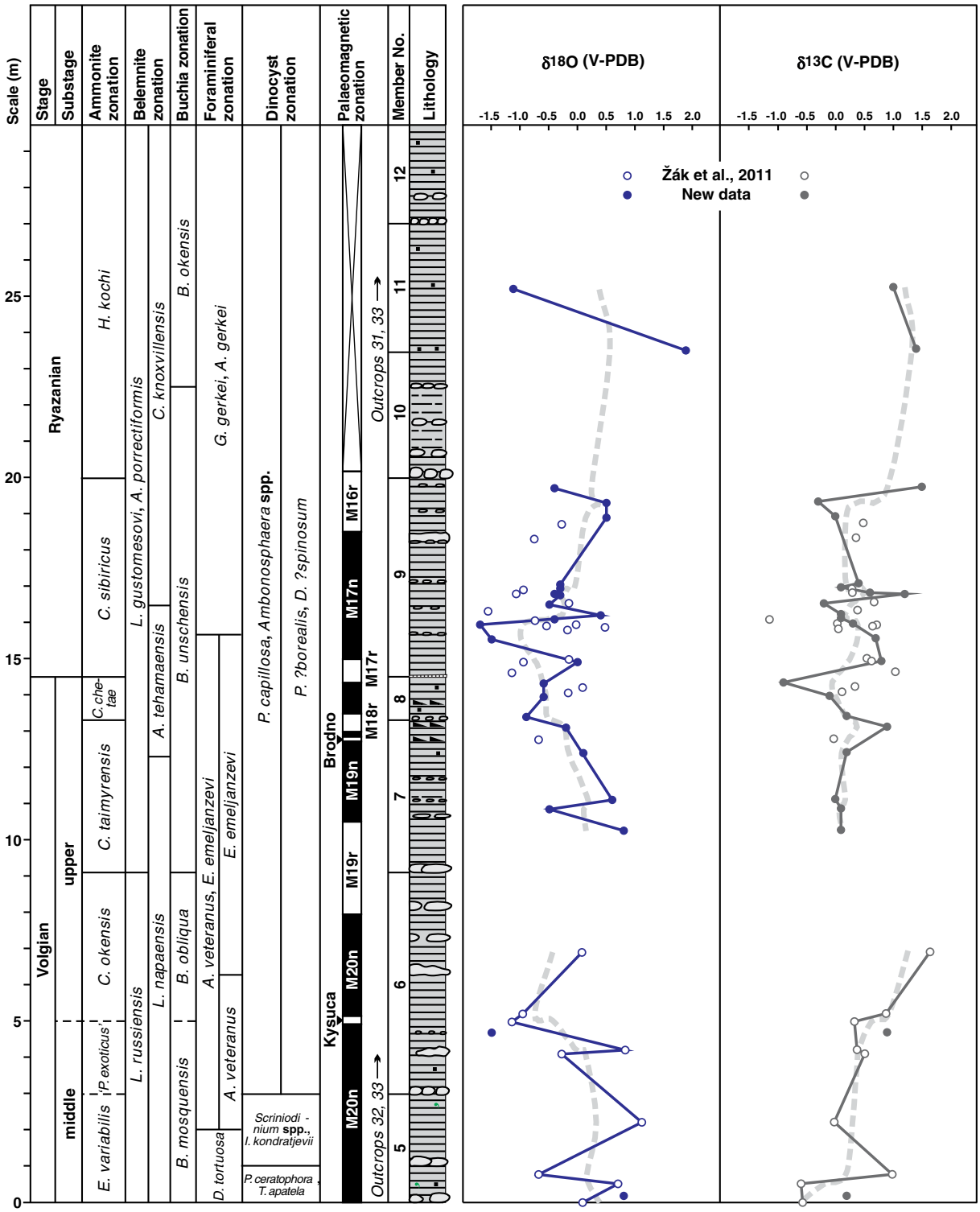

Fig. 6. Stable isotope signals at the Nordvik section (northern East Siberia) after Žák et al. (2011) with some additions. For the interval from the *E. variabilis* Zone to the *C. okensis* Zone, all of the data are summarised using a 5-point moving average. For the interval from the *C. taimyrensis* Zone to the *H. kochi* Zone, only new data are summarised using a 5-point moving average. Biostratigraphy and lithology are after Zakharov et al. (1983), Nikitenko et al. (2008), Zakharov and Rogov (2008), and Dzyuba (2012) (for legend see Fig. 5). The palaeomagnetic zonation is after Houša et al. (2007) with a correction after Bragin et al. (2013).

has long been associated with a mass extinction event (Raup and Sepkoski, 1984), numerous data suggest high biodiversity at this level. High diversity has been reported for plants (Niklas, 1988), tetrapods and insects (Alekseev et al., 2001) on the continents and for ammonites (Rogov et al., 2010), belemnites (Dzyuba, 2013), bivalves and brachiopods (Hammer et al., 2011) in Boreal seas. The following arguments were presented by Rogov et al. (2010) to explain the 'myth' of the J–K boundary extinction phenomena: (1) the fauna of the J–K boundary interval (especially from Boreal basins) were poorly known until recently; (2) the increase of speciation rate and/or provinciality was obscured in the summaries of datasets from all stages/substages and regions; and (3) most of the palaeontological data are from the most-studied regions of Europe, where regressive/terrestrial/freshwater facies around the J–K boundary are widespread.

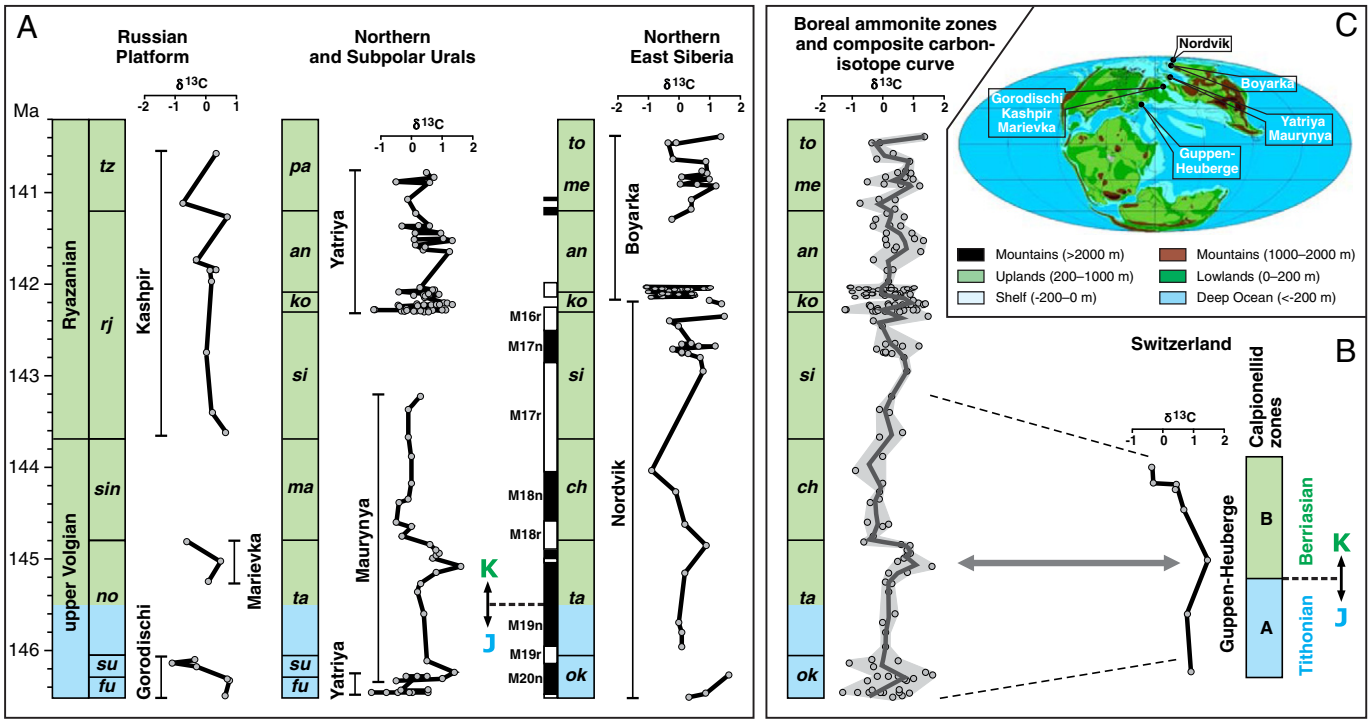

Fig. 7. (A) Carbon isotope excursions across the J–K boundary interval in the Boreal sections: Gorodischi, Kashpir (Gröcke et al., 2003), Marievka (Price and Rogov, 2009), Yatriya (Price and Mutterlose, 2004), Maurynya (present paper), Boyarka (Nunn et al., 2010), Nordvik (Žák et al., 2011, with some additions). (B) Correlation of the Boreal composite (present paper) and Tethyan Guppen-Heuberge (Weissert and Mohr, 1996) carbon-isotope curves. (C) Positions of all of the compared sections on the palaeomap for the Tithonian (Rees et al., 2000). The palaeomagnetic zonation is modified after Houša et al. (2007) according to Bragin et al. (2013). Ammonite zones and beds: *an — Surites analogus, ch — Chetaites chetae, fu — Kachpurites fulgens, ko — Hectoroceras kochi, ma — Subcraspedites maurynijensis, me — Bojarkia mesezhnikowi, no — Craspedites nodiger, ok — Craspedites okensis, pa — Bojarkia payeri, rj — Riasanites rjasanensis, si — Chetaites sibiricus, sin — Volgidiscus singularis, su — Craspedites subditus, ta — Craspedites taimyrensis, to — Tollia tolli, tz — Surites tzikwinianus.*

It is important to note that black organic-rich shales are widespread in the sedimentary record of the Upper Jurassic and part of the Berriasian interval. According to numerous data summarised by Föllmi (2012), Tithonian–Berriasian black shale horizons are found in eastern Antarctica, the Argentinian Neuquén Basin, northeast Mexico, southern England, the Norway–Greenland Seaway and the Barents Sea, the Russian Volga Basin, the West Siberian Basin, the eastern Tethys (Iraq, Himalayas) and Japan. According to Doré (1991), organic-rich shales formed in the Late Jurassic as a result of multiple local mechanisms, such as a strong transgressive regime, limited sea-connections between the northern Tethys and the Boreal basins, reduced clastic input and a globally warm and equable climate, which led to stagnation and a high organic productivity environment in some basins. However, the long-term eustatic curve for the earliest Cretaceous (~145–140 Ma) shows a negative trend (Haq and Al-Qahtani, 2005). Regressive episodes have been documented at the Tithonian–Berriasian transition in Europe (Jacquin et al., 1998) as well as at the Volgian–Ryazanian transition in East Greenland (Surlyk, 1991), the Russian Platform (Sahagian et al., 1996) and the Northern and Subpolar Urals (Golbert et al., 1972; Dzyuba, 2013) but not in northern East Siberia (Zakharov et al., 1994, in press). Föllmi (2012) suggests that the sea level lowstand and arid climate near the J–K boundary caused biogeochemical weathering rates and terrigenous material fluxes into the ocean to decrease. Under such circumstances, the accumulation of organic-rich sediments was promoted by ocean stratification and the resulting dys- to anaerobic conditions in the bottom waters of regional basins. The appearance of organic-rich sediments that were unlikely to settle evenly over geological time or that could be eroded in some areas caused the variations of $\delta^{13}C$ values in the sedimentary record. The variations of $\delta^{13}C$ values near the J–K boundary that we established in the studied sections are evidence of a global perturbation of the carbon isotope cycle at that time.

5.2. Significant carbon isotope excursions and their correlation potential

The Volgian and Ryazanian in Siberia are completely characterised by carbon isotope data; however, only the $\delta^{13}C$ variations for the upper Volgian–Ryazanian interval have been verified in several sections (Fig. 7). A comparison of the obtained carbon-isotope curves for this interval with published data shows that the excursion in the lower part of the Maurynya section is coeval with that of the *Kachpurites fulgens–Craspedites subditus* ammonite Zone transition in the Gorodischi (Gröcke et al., 2003) and Yatriya (Price and Mutterlose, 2004) sections and in the middle part of the *Craspedites okensis* ammonite Zone in the Nordvik section (Žák et al., 2011). A positive excursion that marks the uppermost part of the *Craspedites taimyrensis* ammonite Zone in the Maurynya and Nordvik sections is probably observed in the Marievka section, where it is represented by a single data point within the *Craspedites nodiger* ammonite Zone (Price and Rogov, 2009). Based on its position in the Nordvik section, this positive excursion is defined just above the J–K boundary, which was established here by palaeomagnetic data (Houša et al., 2007). The subsequent decrease in $\delta^{13}C$ values in the *Subcraspedites maurynijensis* ammonite beds of the Maurynya section is isochronal to that in the *Chetaites chetae* ammonite Zone in the Nordvik section.

The Ryazanian carbon-isotope curves also show several oscillations (Fig. 7). Three positive excursions are identified in the Yatriya section (see Fig. 3 of Price and Mutterlose, 2004). The first excursion peak is recorded in the middle part of the *Hectoroceras kochi* ammonite Zone and corresponds with the high carbon isotope values of the mid-*H. kochi* Zone in the Nordvik section. The second positive event is recorded in the middle part of the *Surites analogus* ammonite Zone and is followed by a return to pre-excursion values near the *S. analogus–Bojarkia payeri* ammonite Zone transition. The next shift towards more positive values is seen in the lower part of the *B. payeri* Zone; this Yatriyan shift is also traced in the *Bojarkia*

mesezhnikowi–Tollia tolli ammonite Zones of the Boyarka section (Nunn et al., 2010). The $\delta^{13}C$ record through the Ryazanian of the Kashpir section (Gröcke et al., 2003) has too low a resolution to allow a precise comparison.

The integration of the carbon-isotope data from the sections described above allows a reconstruction of the generalised carbon-isotope curve to be proposed as a composite reference curve for the upper Volgian and Ryazanian in the Boreal regions (Fig. 7). The data from the Maurynya and Nordvik sections obtained during this study that cover the interval from the *Craspedites okensis* to *Chetaites sibiricus* Zones form the basis of this curve. The data from the Yatriya (see Fig. 3 of Price and Mutterlose, 2004) and Boyarka (Nunn et al., 2010) sections are used to define the carbon isotope trends in the overlying interval. It is noteworthy that the composite Tethyan $\delta^{13}C$ curve that is based on bulk carbonate analyses and that was recently revised by Weissert and Erba (2004) is relatively smooth in the Upper Tithonian–Berriasian interval. Nunn et al. (2009, 2010) suggest that such feature, which was observed in other intervals in the Jurassic and Cretaceous, is the result of the mixing of different biogenic components, which will average out natural variations in habitat, vital effects, time and preservation. As a rule, $\delta^{13}C$ values derived from belemnites are considerably more scattered than those in the bulk carbonate record. The composite Boreal and Tethyan $\delta^{13}C$ records of the studied time interval do not contain large differences in the degree of scatter but, for reasons that are not quite clear, most of the Boreal $\delta^{13}C$ excursions are not visible or are strongly smoothed on the published Tethyan $\delta^{13}C$ curves. One $\delta^{13}C$ event is represented on Tethyan curves, and we consider it below.

A comparison of the composite Boreal $\delta^{13}C$ curve with the carbon isotope variations in the Tethyan Guppen-Heuberge pelagic-carbonate section (Switzerland) was performed using magnetostratigraphic data. In the Guppen-Heuberge section, two calpionellid zones (A and B), which correspond to the M20n–M17r interval (Gradstein et al., 2004; Ogg and Ogg, 2008), are recognised in the J–K boundary interval (Weissert and Mohr, 1996). According to Bragin et al. (2013) and Houša et al. (2007), these magnetozones correspond to the interval from the uppermost middle Volgian to the lower part of the Ryazanian *Chetaites sibiricus* ammonite Zone in the Boreal Nordvik section. Because the Guppen-Heuberge and Nordvik sections are both characterised by a significant positive carbon isotope shift just above the J–K boundary followed by a rapid return to pre-excursion values, this isotopic event can be assumed to be widespread. Therefore, this positive C-isotope excursion, which is most distinctively observed in the Maurynya section but is also (less obviously) found in the Marievka section (Fig. 7), could not have been caused solely by local oceanographic conditions; rather, it may reflect global variations of the dissolved inorganic carbon isotopic composition in the earliest Berriasian seawater, which in turn can be interpreted as a response to increased organic-carbon burial in the Boreal and other basins.

Moreover, this positive excursion, which begins in the top part of the Boreal *Craspedites taimyrensis* ammonite Zone and returns to pre-excursion values at the *C. taimyrensis–Chetaites chetae* zonal boundary, is significant for the Boreal–Tethyan correlation of the J–K boundary strata. If the base of the *C. chetae* ammonite Zone is inside magnetozone M18r (Houša et al., 2007; Bragin et al., 2013), it could be approximately aligned with the base of the Tethyan *Pseudosubplanites grandis* ammonite Subzone, which is located within the same palaeomagnetic zone (Gradstein et al., 2004; Ogg and Ogg, 2008; Guzhikov et al., 2012). During the 80 years before the Lyon-Neuchâtel 'Colloque sur la limite Jurassique–Crétacé' of 1973 (Flandrin et al., 1975), the boundary that corresponds to the base of the *P. grandis* Subzone in the modern ammonite scale was considered as marking the J–K boundary. Based on recent bio- and magnetostratigraphic data and carbon isotope records, that boundary may be the most optimal position for the J-K boundary.

The base of the *Pseudosubplanites grandis* Subzone meets the many requirements for marking the J–K boundary. First, this boundary was established by ammonoids, which are the main group used for precise subdivisions and correlations in the Mesozoic. Second, this boundary is located within the traditional basal Berriasian interval (Wimbledon et al., 2011). Third, it can be recognised in field observations (e.g., Guzhikov et al., 2012). Although this boundary is not characterised by significant faunal changes, which has been cause for objections from the IUGS Lower Cretaceous Ammonite Working Group, i.e., the 'Kilian group' (Hoedemaeker et al., 1993), the other palaeontological markers in the traditional basal Berriasian interval have less correlation potential. In our opinion, one of the most important criteria for defining the stratigraphic position of the J–K boundary is the possibility of tracing this boundary to the Boreal sections. As mentioned above, an approximate correspondence between the base of the *P. grandis* Subzone and the base of the Boreal *Chetaites chetae* Zone has been demonstrated by magnetostratigraphic data. In this study, a distinct carbon isotope marker was established near this level, and this marker could probably be detected in several other Tethyan sections.

6. Conclusions

Detailed $\delta^{13}C$ and $\delta^{18}O$ curves are constructed for the Maurynya section (eastern slope of the Northern Urals, Western Siberia) and are updated for the Nordvik section (Laptev Sea, northern East Siberia) based on geochemical isotope analyses of Boreal belemnite (Cylindroteuthididae) rostra from the J–K boundary strata. The Maurynya and Nordvik carbon isotope records have similar absolute $\delta^{13}C$ values and variations, and the biostratigraphically-correlated curves have similar patterns. The lower $\delta^{18}O$ values obtained for the Maurynya section in comparison with the data from the Nordvik section indicate slightly higher temperatures in the basin where the Maurynya section was deposited that correlates well with its palaeogeographic position.

A comparison of the reconstructed carbon-isotope curves for the Maurynya and Nordvik sections with similar curves from other Boreal sections (1) reveals correlatable excursions in the J–K boundary interval, and (2) allows the creation of a Boreal composite carbon-isotope curve that characterises the upper Volgian and Ryazanian in detail. In the interval from the *Craspedites okensis* Zone to the *Chetaites sibiricus* Zone, this curve was reconstructed using the data from the Maurynya and Nordvik sections. For the overlying sediments, we used data from the Yatriya and Boyarka sections. We interpret all of the significant shifts in $\delta^{13}C$ values as reflecting changes in the organic carbon burial rates.

One of the most remarkable positive $\delta^{13}C$ excursions in the Boreal curve is recorded in the top part of the upper Volgian *Craspedites taimyrensis* ammonite Zone slightly above the J–K boundary, which is established here by palaeomagnetic data. In the Tethyan Guppen-Heuberge pelagic-carbonate section (Switzerland), a significant positive shift is observed slightly above the base of the *Calpionella* Zone (B Zone), which corresponds approximately to the J–K boundary. The $\delta^{13}C$ event recognised in this study could be a useful marker for the Panboreal and Boreal–Tethyan correlation of J–K boundary beds.

Acknowledgements

This is a contribution to the Russian Academy of Sciences Programs 23 and 28 and financially supported by the grant from the Russian Foundation for Basic Researches No. 12-05-00453. We thank the editor F. Surlyk for useful comments. Two anonymous reviewers are thanked for constructive reviews. We thank E.M. Khabarov and H. Wierzbowski for their recommendations concerning the use of analytical methods. We are grateful to M.A. Rogov, D.A. Ruban and V.A. Zakharov for their support with literature and useful discussion. Additional thanks are addressed to A.S. Alifirov, A.E. Igolnikov, V.A. Marinov, O.S. Urman and P.A. Yan for their assistance during field work and to D.V. Grazhdankin for his help with translation.

Appendix A. Supplementary data

Supplementary data associated with this article can be found in the online version, at http://dx.doi.org/10.1016/j.palaeo.2013.04.013. These data include Google maps of the most important areas described in this article.

References

Abbink, O., Targarona, J., Brinkhuis, H., Visscher, H., 2001. Late Jurassic to earliest Cretaceous palaeoclimatic evolution of the Northern Sea. Global and Planetary Change 30, 231–256.

Alekseev, A.S., Dmitriev, V.Yu., Ponomarenko, A.G., 2001. Evolution of the Taxonomic Diversity. GEOS, Moscow (126 pp. (in Russian)).

Alifirov, A.S., Igolnikov, A.E., Dzyuba, O.S., 2008. Ammonites and structure of Volgian–Berriasian beds in the Mauryniya section (Subpolar Urals): new data. In: Dzyuba, O.S., Zakharov, V.A., Shurygin, B.N. (Eds.), Cretaceous System of Russia and Adjacent Countries: Problems of Stratigraphy and Paleogeography: Proceeding of the Fourth All-Russian Meeting, Novosibirsk, September 19–23, 2008. Publishing House SB RAS, Novosibirsk, pp. 20–23 (in Russian).

Anderson, T.F., Popp, B.N., Williams, A.C., Ho, L.Z., Hudson, J.D., 1994. The stable isotopic record of fossils from the Petersborough Member, Oxford Clay Formation (Jurassic), UK: palaeoenvironmental implications. Journal of the Geological Society of London 151, 125–138.

Baraboshkin, E.J., 2004. Lower Cretaceous Zonal standard of the Boreal Realm. Bulletin of the Moscow Society of Naturalists, Series Geology 79, 44–68 (in Russian with English abstract).

Bragin, V.Yu., Dzyuba, O.S., Kazansky, A.Yu., Shurygin, B.N., 2013. New data on the magnetostratigraphy of the Jurassic–Cretaceous boundary interval, Nordvik Peninsula (northern East Siberia). Russian Geology and Geophysics 54, 329–342.

Brand, U., Veiser, J., 1980. Chemical diagenesis of a multicomponent carbonate system — 1. Trace element. Journal of Sedimentary Petrology 50, 1219–1236.

Callomon, J.H., Birkelund, T., 1982. The ammonite zones of the Boreal Volgian (Upper Jurassic) in East Greenland. In: Embry, A.F., Balkwill, H.R. (Eds.), Arctic Geology and Geophysics: Canadian Society of Petroleum Geologists, Memoir, 8, pp. 349–369.

Casey, R., Mesezhnikov, M.S., Shulgina, N.I., 1988. Ammonite zones in Jurassic–Cretaceous boundary sediments of the Boreal Realm. Bulletin of the Academy of Sciences of the U.S.S.R. Geologic Series 10, 71–84 (in Russian).

Dera, G., Brigaud, B., Monna, F., Laffont, R., Pucéat, E., Deconinck, J.-F., Pellenard, P., Joachimski, M.M., Durlet, C., 2011. Climatic ups and downs in a disturbed Jurassic world. Geology 39, 215–218.

Ditchfield, P.W., 1997. High northern palaeolatitude Jurassic–Cretaceous palaeotemperature variation: new data from Kong Karls Land, Svalbard. Palaeogeography, Palaeoclimatology, Palaeoecology 130, 163–175.

Doré, A.G., 1991. The structural foundation and evolution of Mesozoic seaways between Europe and the Arctic. Palaeogeography, Palaeoclimatology, Palaeoecology 87, 441–492.

Dzyuba, O.S., 2012. Belemnites and biostratigraphy of the Jurassic–Cretaceous boundary deposits of northern East Siberia: new data on the Nordvik Peninsula. Stratigraphy and Geological Correlation 20, 53–72.

Dzyuba, O.S., 2013. Belemnites in the Jurassic–Cretaceous boundary interval of the Maurynya and Yatriya River sections, Western Siberia: biostratigraphic significance and dynamics of taxonomic diversity. Stratigraphy and Geological Correlation 21, 189–214.

Emmanuel, L., Renard, M., 1993. Carbonate geochemistry (Mn, $d^{13}C$, $d^{18}O$) of the late Tithonian–Berriasian pelagic limestones of the Vocontian trough (SE France). Bulletin de Centre de Recherches et Exploration–Production Elf-Aquitaine 17, 205–221.

Flandrin, J., Schaer, J.P., Enay, R., Remane, J., Rio, M., Kubler, B., Le Hégarat, G., Mouterde, R., Thieuloy, J.P., 1975. Discussion générale préliminaire au dépôt des motions. Colloque sur la limite Jurassique–Crétacé, Lyon–Neuchâtel, September 1973: Mémoires du Bureau de Recherches Géologiques et Miniéres, 86, pp. 386–393.

Föllmi, K.B., 2012. Early Cretaceous life, climate and anoxia. Cretaceous Research 35, 230–257.

Golbert, A.V., Klimova, I.G., Saks, V.N., 1972. The Neocomian Reference Section in the Subpolar Trans-Urals, Western Siberia. Nauka, Novosibirsk (184 pp. (in Russian)).

Grabowski, J., Michalík, J., Pszczółkowski, A., Lintnerová, O., 2010. Magneto-, and isotope stratigraphy around the Jurassic/Cretaceous boundary in the Vysoká Unit (Malé Karpaty Mountains, Slovakia): correlations and tectonic implications. Geologica Carpathica 61, 309–326.

Gradstein, F.M., Ogg, J.G., Smith, A.G. (Eds.), 2004. A Geologic Time Scale 2004. Cambridge University Press, Cambridge, U.K.

Gradstein, F.M., Ogg, J.G., Schmitz, M.D., Ogg, G.M. (Eds.), 2012. The Geologic Time Scale 2012, first ed. Elsevier BV.

Gröcke, D.R., Price, G.D., Ruffell, A.H., Mutterlose, J., Baraboshkin, E., 2003. Isotopic evidence for Late Jurassic–Early Cretaceous climate change. Palaeogeography, Palaeoclimatology, Palaeoecology 202, 97–118.

Gurari, F.G. (Ed.), 2004. A Decision of the 6th Interdepartmental Stratigraphical Meeting on Consideration and Arrival of the Improved Stratigraphical Scales of the Mesozoic Deposits of West Siberia. SNIIGGiMS, Novosibirsk (in Russian).

Gustomesov, V.A., 1976. Belemnites and their relationships with facies and habitat basin development. Bulletin of the Moscow Society of Naturalists, Series Geology 51, 107–117 (in Russian).

Guzhikov, A.Yu., Arkad'ev, V.V., Baraboshkin, E.Yu., Bagaeva, M.I., Piskunov, V.K., Rud'ko, S.V., Perminov, V.A., Manikin, A.G., 2012. New sedimentological, bio-, and magnetostratigraphic data on the Jurassic–Cretaceous boundary Interval of Eastern Crimea (Feodosiya). Stratigraphy and Geological Correlation 20, 261–294.

Hammer, Ø., Nakrem, H.A., Little, C.T.S., Hryniewicz, K., Sandy, M.R., Hurum, J.H., Druckenmiller, P., Knutsen, E.M., Høyberget, M., 2011. Hydrocarbon seeps from close to the Jurassic–Cretaceous boundary, Svalbard. Palaeogeography, Palaeoclimatology, Palaeoecology 306, 15–26.

Hammer, Ø., Collignon, M., Nakrem, H.A., 2012. Organic carbon isotope chemostratigraphy and cyclostratigraphy in the Volgian of Svalbard. Norwegian Journal of Geology 92, 103–112.

Haq, B.U., Al-Qahtani, A.M., 2005. Phanerozoic cycles of sea-level change on the Arabian Platform. GeoArabia 10, 127–160.

Hardenbol, J., Thierry, J., Farley, M.B., Jacquin, T., Graciansky, P.-C., de Vail, P.R., 1998. Mesozoic and Cenozoic sequence chronostratigraphic framework of European Basins. In: Graciansky, P.-C., de Hardenbol, J., Jacquin, T., Vail, P.R. (Eds.), Mesozoic and Cenozoic Sequence Stratigraphy of European Basins: SEPM Special Publication, 60, pp. 3–13.

Hoedemaeker, P.J., Company, M., (reporters), Aguirre-Urreta, M.B., Avram, E., Bogdanova, T.N., Bujtor, L., Bulot, L., Cecca, F., Delanoy, G., Ettachfini, M., Memmi, L., Owen, H.G., Rawson, P.F., Sandoval, J., Tavera, J.M., Thieuloy, J.P., Tovbina, S.Z., Vašíček, Z., 1993. Ammonite zonation for the Lower Cretaceous of the Mediterranean region; basis for the stratigraphic correlation within IGCP-Project 262. Revista Espanola de Paleontologia 8, 117–120.

Hoedemaeker, P.J., Reboulet, S. (reporters), Aguirre-Urreta, M.B., Alsen, P., Aoutem, M., Atrops, F., Barragan, R., Company, M., Gonza' lez Arreola, C., Klein, J., Lukeneder, A., Ploch, I., Raisossadat, N., Rawson, P.F., Ropolo, P., Vašíček, Z., Vermeulen, J., Wippich, M., 2003. Report on the 1st International Workshop of the IUGS Lower Cretaceous Ammonite Working Group, the 'Kilian Group' (Lyon, 11 July 2002). Cretaceous Research 24, 89–94 and erratum (p. 805).

Houša, V., Pruner, P., Zakharov, V.A., Kostak, M., Chadima, M., Rogov, M.A., Šlechta, S., Mazuch, M., 2007. Boreal–Tethyan correlation of the Jurassic–Cretaceous boundary interval by magneto- and biostratigraphy. Stratigraphy and Geological Correlation 15, 297–309.

Huang, C.M., Retallack, G.J., Wang, C.S., 2012. Early Cretaceous atmospheric pCO_2 levels recorded from pedogenic carbonates in China. Cretaceous Research 33, 42–49.

Jacquin, T., Dardeau, G., Durlet, C., de Graciansky, P.-C., Hantzpergue, P., 1998. The North Sea Cycle: an overview of 2nd-order transgressive/regressive facies cycles in Western Europe. In: Graciansky, P.-C., de Hardenbol, J., Jacquin, T., Vail, P.R. (Eds.), Mesozoic and Cenozoic Sequence Stratigraphy of European Basins: SEPM Special Publication, 60, pp. 445–466.

Jeletzky, J.A., 1984. Jurassic–Cretaceous boundary beds of Western and Arctic Canada and the problem of the Tithonian–Berriasian stages in the Boreal Realm. Geological Association of Canada Special Paper 27, 175–255.

Jenkyns, H.C., Jones, C.E., Gröcke, D.R., Hesselbo, S.P., Parkinson, D.N., 2002. Chemostratigraphy of the Jurassic System: applications, limitations and implications for palaeoceanography. Journal of the Geological Society of London 159, 351–378.

Kiselev, D.N., 2003. Seltzo-Voskresenskoe. In: Kiselev, D.N., Baranov, V.N., Muravin, E.S., Novikov, I.V., Sennikov, A.G. (Eds.), Atlas of the Yaroslavl Region Geological Monuments. Izd-vo YGPU, Yaroslavl, pp. 58–62 (in Russian).

Machel, H.G., 1985. Cathodoluminescence in calcite and dolomite and its chemical interpretation. Geoscience Canada 12, 139–147.

McArthur, J.M., Mutterlose, J., Price, G.D., Rawson, P.F., Ruffell, A., Thirlwall, M.F., 2004. Belemnites of Valanginian, Hauterivian and Barremian age: Sr-isotope stratigraphy, composition ($^{87}Sr/^{86}Sr$, $\delta^{13}C$, $\delta^{18}O$, Na, Sr, Mg), and palaeo-oceanography. Palaeogeography, Palaeoclimatology, Palaeoecology 202, 253–272.

Mesezhnikov, M.S., 1989. Tithonian, Volgian and Portlandian stages (geological and biological events, correlation). In: Sokolov, B.S. (Ed.), Sedimentary Cover of the Earth in Space and Time. : Stratigraphy and paleontology. Nauka, Moscow, pp. 100–107 (in Russian with English abstract).

Michalík, J., Reháková, D., Halásová, E., Lintnerová, O., 2009. The Brodno section — a potential regional stratotype of the Jurassic/Cretaceous boundary (Western Carpathians). Geologica Carpathica 60, 213–232.

Mitta, V.V., 2007. Ammonite assemblages from basal layers of the Ryazanian Stage (Lower Cretaceous) of Central Russia. Stratigraphy and Geological Correlation 15, 193–205.

Mitta, V.V., 2008. Ammonites of Tethyan origin from the Ryazanian of the Russian Platform: genus *Riasanites* Spath. Paleontological Journal 42, 251–259.

Mitta, V.V., 2010. Late Volgian *Kachpurites* Spath (Craspeditidae, Ammonoidea) of the Russian Platform. Paleontological Journal 44, 622–631.

Mitta, V.V., 2011. Ammonites of Tethyan origin in the Ryazanian Stage of the Russian Platform: genus *Mazenoticeras* and other Neocomitidae. Paleontological Journal 45, 143–153.

Mitta, V.V., Sha, J., 2011. Ammonite distribution across the Jurassic–Cretaceous boundary in Central Russia. Paleontological Journal 45, 379–389.

Mutterlose, J., 1983. Phylogenie und Biostratigraphie der Unterfamilie Oxytheutinae (Belemnitida) aus dem Barrême (Unter-Kreide) NW-Europas. Palaeontographica 180, 1–90.

Mutterlose, J., Kessels, K., 2000. Early Cretaceous calcareous nannofossils from high latitudes: implications for palaeobiogeography and palaeoclimate. Palaeogeography, Palaeoclimatology, Palaeoecology 160, 347–372.

Mutterlose, J., Malkoc, M., Schouten, S., Sinninghe Damsté, J.S., Forster, A., 2010. TEX_{86} and stable $\delta^{18}O$ paleothermometry of early Cretaceous sediments: Implications for belemnite ecology and paleotemperature proxy application. Earth and Planetary Science Letters 298, 286–298.

Newman, M., 2001. A new picture of life's history on Earth. PNAS 98, 5955–5956.

Niebuhr, B., Joachimski, M.M., 2002. Stable isotope and trace element geochemistry of Upper Cretaceous carbonates and belemnite rostra (Middle Campanian, north Germany). Geobios 35, 51–64.
Nikitenko, B.I., Pestchevitskaya, E.B., Lebedeva, N.K., Ilyina, V.I., 2008. Micropaleontological and palynological analyses across the Jurassic–Cretaceous boundary on Nordvik Peninsula, Northeast Siberia. Newsletters on Stratigraphy 42, 181–222.
Niklas, K.J., 1988. Patterns of vascular plant diversification in the fossil record: proof and conjecture. Annals of the Missouri Botanical Garden 75, 35–54.
Nunn, E.V., Price, G.D., 2010. Late Jurassic (Kimmeridgian–Tithonian) stable isotopes (δ18O, δ13C) and Mg/Ca ratios: New palaeoclimate data from Helmsdale, northeast Scotland. Palaeogeography, Palaeoclimatology, Palaeoecology 292, 321–335.
Nunn, E.V., Price, G.D., Hart, M.B., Page, K.N., Leng, M.J., 2009. Isotopic signals from Callovian–Kimmeridgian (Middle–Upper Jurassic) belemnites and bulk organic carbon, Staffin Bay, Isle of Skye, Scotland. Journal of the Geological Society of London 166, 633–641.
Nunn, E.V., Price, G.D., Gröcke, D.R., Baraboshkin, E.Y., Leng, M.J., Hart, M.B., 2010. The Valanginian positive carbon isotope event in Arctic Russia: evidence from terrestrial and marine isotope records and implications for global carbon cycling. Cretaceous Research 31, 577–592.
Ogg, J., Ogg, G., 2008. Late Jurassic (139–169 Ma time-slice). http://www.nhm.uio.no/norges/timescale/5_JurCret_Sept08.pdf.
Ogg, J.G., Hasenyager, R.W., Wimbledon, W.A., Channel, J.E.T., Bralower, T.J., 1991. Magnetostratigraphy of the Jurassic–Cretaceous boundary interval — Tethyan and English faunal realms. Cretaceous Research 12, 455–482.
Oschmann, W., Röhl, J., Schmid-Röhl, A., Seilacher, A., 1999. Der Posidonienschiefer (Toarcium, Unterer Jura) von Dotternhausen. Jahresberichte und Mitteilungen des Oberrheinischen Geologischen Vereines 81, 231–255.
Podlaha, O.G., Mutterlose, J., Veizer, J., 1998. Preservation of $\delta^{18}O$ and $\delta^{13}C$ in belemnite rostra from the Jurassic/Early Cretaceous successions. American Journal of Science 298, 324–347.
Price, G.D., Mutterlose, J., 2004. Isotopic signals from the late Jurassic–early Cretaceous (Volgian–Valanginian) sub-Arctic belemnites, Yatria River, Western Siberia. Journal of the Geological Society of London 161, 959–968.
Price, G.D., Rogov, M.A., 2009. An isotopic appraisal of the Late Jurassic greenhouse phase in the Russian platform. Palaeogeography, Palaeoclimatology, Palaeoecology 273, 41–49.
Price, G.D., Sellwood, B.W., 1997. 'Warm' palaeotemperatures from high Late Jurassic palaeolatitudes (Falkland Plateau): Ecological, environmental or diagenetic controls? Palaeogeography, Palaeoclimatology, Palaeoecology 129, 315–327.
Price, G.D., Ruffell, A.H., Jones, C.E., Kalin, R.M., Mutterlose, J., 2000. Isotopic evidence for temperature variation during the early Cretaceous (late Ryazanian–mid Hauterivian). Journal of the Geological Society of London 157, 335–343.
Pruner, P., Houša, V., Olóriz, F., Košťák, M., Krs, M., Man, O., Schnabl, P., Venhodová, D., Tavera, J.M., Mazuch, M., 2010. High-resolution magnetostratigraphy and biostratigraphic zonation of the Jurassic/Cretaceous boundary strata in the Puerto Escaño section (southern Spain). Cretaceous Research 31, 192–206.
Raup, D., Sepkoski, J., 1984. Periodicity of extinctions in the geologic past. Proceedings of the National Academy of Sciences USA 81, 801–805.
Rees, P. McA, Ziegler, A.M., Valdes, P.J., 2000. Jurassic phytogeography and climates: new data and model comparisons. In: Huber, B.T., Macleod, K.G., Wing, S.L. (Eds.), Warm Climates in Earth History. Cambridge University Press, Cambridge, pp. 297–318.
Remane, J., 1991. The Jurassic–Cretaceous boundary: problems of definition and procedure. Cretaceous Research 12, 447–453.
Rexfort, A., Mutterlose, J., 2009. The role of biogeography and ecology on the isotope signature of cuttlefishes (Cephalopoda, Sepiidae) and the impact on belemnite studies. Palaeogeography, Palaeoclimatology, Palaeoecology 284, 153–163.
Rogov, M.A., 2010. New data on ammonites and stratigraphy of the Volgian stage in Spitzbergen. Stratigraphy and Geological Correlation 18, 505–531.
Rogov, M.A., Zakharov, V.A., 2009. Ammonite- and bivalve-based biostratigraphy and Panboreal correlation of the Volgian Stage. Science in China Series D: Earth Sciences 52, 1890–1909.
Rogov, M.A., Zakharov, V.A., Nikitenko, B.L., 2010. The Jurassic–Cretaceous boundary problem and the myth on J/K boundary extinction. Earth Science Frontiers 17 (Special Issue), 13–14.
Rosales, I., Quesada, S., Robles, S., 2001. Primary and diagenetic isotopic signals in fossils and hemipelagic carbonates: the Lower Jurassic of northern Spain. Sedimentology 48, 1149–1169.
Rosales, I., Quesada, S., Robles, S., 2004. Paleotemperature variations of Early Jurassic seawater recorded in geochemical trends of belemnites from the Basque-Cantabrian basin, northern Spain. Palaeogeography, Palaeoclimatology, Palaeoecology 203, 253–275.
Ruffell, A.H., Price, G.D., Mutterlose, J., Kessels, K., Baraboshkin, E., Gröcke, D.R., 2002. Palaeoclimate indicators (clay minerals, calcareous nannofossils, stable isotopes) compared from two successions in the late Jurassic of the Volga Basin (SE Russia). Geological Journal 37, 17–33.
Sælen, G., Doyle, P., Talbot, M.R., 1996. Stable-isotope analyses of belemnite rostra from the Whitby Mudstone Fm, England: surface water conditions during deposition of a marine black shale. Palaios 11, 97–117.
Sahagian, D., Pinous, O., Olferiev, A., Zakharov, V., 1996. Eustatic curve for the Middle Jurassic–Cretaceous based on Russian Platform and Siberian stratigraphy: zonal resolution. AAPG Bulletin 80, 1433–1458.
Saks, V.N. (Ed.), 1975. The Jurassic–Cretaceous Boundary and the Berriasian Stage in the Boreal Realm. Keter, Jerusalem.
Savary, B., Cecca, F., Bartolini, A., 2003. Étude stratigraphique du Rosso Ammonitico du Monte Inici (domaine Trapanais, Sicile occidentale): événements biosédimentaires au Jurassique moyen-Crétacé inférieur. Geodiversitas 25, 217–235.
Schnyder, J., Ruffell, A., Deconinck, J.-F., Baudin, F., 2006. Conjunctive use of spectral gamma-ray logs and clay mineralogy in defining late Jurassic–early Cretaceous palaeoclimate change (Dorset, U.K.). Palaeogeography, Palaeoclimatology, Palaeoecology 229, 303–320.
Schnyder, J., Baudin, F., Deconinck, J.-F., 2009. Occurrence of organic-matter-rich beds in Early Cretaceous coastal evaporitic setting (Dorset, UK): a link to long-term palaeoclimate changes? Cretaceous Research 30, 356–366.
Seilacher, A., Reif, W.-E., Westphal, F., 1985. Sedimentological, ecological and temporal patterns of Fossillagerstätten. Philosophical Transactions of the Royal Society of London B 311, 5–24.
Sey, I.I., Kalacheva, E.D., 1999. Lower Berriasian of Southern Primorye (Far East Russia) and the problem of Boreal–Tethyan correlation. Palaeogeography, Palaeoclimatology, Palaeoecology 150, 49–63.
Sha, J.G., Matsukawa, M., Cai, H.W., Jiang, B.Y., Ito, M., He, C.Q., Gu, Z.W., 2003. The Upper Jurassic–Lower Cretaceous of eastern Heilongjiang, northeast China: stratigraphy and regional basin history. Cretaceous Research 24, 715–728.
Sha, J., Chen, S., Cai, H., Jiang, B., Yao, X., Pan, Y., Wang, J., Zhu, Y., He, C., 2006. Jurassic–Cretaceous boundary in northeastern China: placement based on buchiid bivalves and dinoflagellate cysts. Progress in Natural Science 16 (Special Issue), 39–49.
Shurygin, B.N., Nikitenko, B.L., Devyatov, V.P., Il'ina, V.I., Meledina, S.V., Gaideburova, E.A., Dzyuba, O.S., Kazakov, A.M., Mogucheva, N.K., 2000. Stratigraphy of Oil and Gas Basins of Siberia: The Jurassic System. Publishing house of SB RAS, Department 'Geo', Novosibirsk (480 pp. (in Russian with English summary)).
Shurygin, B.N., Nikitenko, B.L., Meledina, S.V., Dzyuba, O.S., Knyazev, V.G., 2011. Comprehensive zonal subdivisions of Siberian Jurassic and their significance for Circum-Arctic correlations. Russian Geology and Geophysics 52, 825–844.
Smith, A.G., Smith, D.G., Funnell, B.M., 1994. Atlas of Mesozoic and Cenozoic Coastlines. Cambridge University Press, Cambridge.
Surlyk, F., 1991. Sequence stratigraphy of the Jurassic–lowermost Cretaceous in East Greenland. AAPG Bulletin 75, 1468–1488.
Surlyk, F., Zakharov, V.A., 1982. Buchiid bivalves from the Upper Jurassic and Lower Cretaceous of East Greenland. Palaeontology 25, 727–753.
Surlyk, F., Callomon, J.H., Bromley, R.G., Birkelund, T., 1973. Stratigraphy of the Jurassic–Lower Cretaceous sediments of Jameson Land and Scoresby Land, East Greenland. Grønlands Geologiske Undersøgelse Bulletin 105, 1–76.
Tremolada, F., Bornemann, A., Bralower, T., Koeberl, C., van de Schootbrugge, B., 2006. Paleoceanographic changes across the Jurassic/Cretaceous boundary: the calcareous phytoplankton response. Earth and Planetary Science Letters 241, 361–371.
Veizer, J., 1983. Chemical diagenesis of carbonates: theory and application of trace elements technique. In: Arthur, M.A., Anderson, T.F., Kaplan, I.R., Veizer, J., Land, L.S. (Eds.), Stable Isotopes in Sedimentary Geology: SEPM Short Course, 10, pp. 3–100.
Vinogradov, V.I., 2009. Possibilities and limitations of isotopic chemostratigraphy. Lithology and Mineral Resources 44, 245–257.
Wang, F., Zhou, X.-H., Zhang, L.-C., Ying, J.-F., Zhang, Y.-T., Wu, F.-Y., Zhu, R.-X., 2006. Late Mesozoic volcanism in the Great Xing'an Range (NE China): timing and implications for the dynamic setting of NE Asia. Earth and Planetary Science Letters 251, 179–198.
Weissert, H., Channell, J.E.T., 1989. Tethyan carbonate carbon isotope stratigraphy across the Jurassic–Cretaceous boundary: an indicator of decelerated global carbon cycling? Paleoceanography 4, 483–494.
Weissert, H., Erba, E., 2004. Volcanism, CO_2 and palaeoclimate: a Late Jurassic–Early Cretaceous carbon and oxygen isotope record. Journal of the Geological Society 161, 695–702.
Weissert, H., Lini, A., 1991. Ice age interludes during the time of Cretaceous greenhouse climate? In: Müller, D.W., McKenzie, J.A., Weissert, H. (Eds.), Controversies in Modern Geology. Academic Press, pp. 173–191.
Weissert, H., Mohr, H., 1996. Late Jurassic climate and its impact on carbon cycling. Palaeogeography, Palaeoclimatology, Palaeoecology 122, 27–43.
Wierzbowski, H., 2002. Detailed oxygen and carbon isotope stratigraphy of the Oxfordian in Central Poland. International Journal of Earth Sciences (Geologische Rundschau) 91, 304–314.
Wierzbowski, H., Joachimski, M., 2007. Reconstruction of late Bajocian–Bathonian marine palaeoenvironments using carbon and oxygen isotope ratios of calcareous fossils from the Polish Jura Chain (central Poland). Palaeogeography, Palaeoclimatology, Palaeoecology 254, 523–540.
Wierzbowski, H., Rogov, M., 2011. Reconstructing the palaeoenvironment of the Middle Russian Sea during the Middle–Late Jurassic transition using stable isotope ratios of cephalopod shells and variations in faunal assemblages. Palaeogeography, Palaeoclimatology, Palaeoecology 299, 250–264.
Wimbledon, W.A.P., 2008. The Jurassic–Cretaceous boundary. An age-old correlative enigma. Episodes 31, 423–428.
Wimbledon, W.A.P., Casellato, C.E., Reháková, D., Bulot, L.G., Erba, E., Gardin, S., Verreussel, R.M.C.H., Munsterman, D.K., Hunt, C.O., 2011. Fixing a basal Berriasian and Jurassic/Cretaceous (J/K) boundary — is there perhaps some light at the end of the tunnel? Rivista Italiana di Paleontologia e Stratigrafia 117, 295–307.
Wimbledon, W.A.P., Reháková, D., Pszczółkowski, A., Casellato, C.E., Halásová, E., Frau, C., Bulot, L.G., Grabowski, J., Sobień, K., Pruner, P., Schnabl, P., Čížková, K., 2013. An account of the bio- and magnetostratigraphy of the upper Tithonian–lower Berriasian interval at Le Chouet, Drôme (SE France). Geologica Carpathica (in press).
Žák, K., Košťák, M., Man, O., Zakharov, V.A., Rogov, M.A., Pruner, P., Dzyuba, O.S., Rohovec, J., Mazuch, M., 2011. Comparison of carbonate C and O stable isotope records across the Jurassic/Cretaceous boundary in the Boreal and Tethyan Realms. Palaeogeography, Palaeoclimatology, Palaeoecology 299, 83–96.
Zakharov, V.A., 1987. The Bivalve Buchia and the Jurassic–Cretaceous Boundary in the Boreal Province. Cretaceous Research 8, 141–153.

Zakharov, V.A., 2011. The Jurassic–Cretaceous boundary and Berriasian GSSP: is there light at the end of the tunnel? (Comments to proposals on the Jurassic–Cretaceous boundary by Berriasian Working Group). News of paleontology and stratigraphy 16–17 (supplement to Russian Geology and Geophysics 52), 69–86 (in Russian with English summary).

Zakharov, V.A., Beizel, A.L., Bogomolov, Yu.I., Konstantinov, A.G., Kurushin, N.I., Meledina, S.V., Nikitenko, B.L., Shurygin, B.N., 1994. Phases and periods in the sea ecosystem evolution in the Boreal Mesozoic. In: Rozanov, A.Yu, Semikhatov, M.A. (Eds.), Ecosystem restructures and the evolution of biosphere, 1, pp. 138–151 (Nedra, Moscow, in Russian).

Zakharov, V.A., Judovnyi, E.G., 1974. Sedimentary process and environmental conditions of fauna in the Khatanga Early Cretaceous Sea. In: Dagis, A.S., Zakharov, V.A. (Eds.), Mesozoic Palaeobiogeography of the North of Eurasia. Nauka, Novosibirsk, pp. 127–174 (in Russian).

Zakharov, V.A., Rogov, M.A., 2008. The upper Volgian Substage in Northeast Siberia (Nordvik Peninsula) and its panboreal correlation based on ammonites. Stratigraphy and Geological Correlation 16, 423–436.

Zakharov, V.A., Nalnyaeva, T.I., Shulgina, N.I., 1983. New data on the biostratigraphy of the Upper Jurassic and Lower Cretaceous deposits on Paksa peninsula, Anabar embayment (north of the Middle Siberia). In: Zakharov, V.A. (Ed.), Jurassic and Cretaceous paleobiogeography and biostratigraphy of Siberia. Nauka, Moscow, pp. 56–99 (in Russian).

Zakharov, V.A., Bogomolov, Yu.I., Il'ina, V.I., Konstantinov, A.G., Kurushin, N.I., Lebedeva, N.K., Meledina, S.V., Nikitenko, B.L., Sobolev, E.S., Shurygin, B.N., 1997. Boreal zonal standard and biostratigraphy of the Siberian Mesozoic. Russian Geology and Geophysics 38, 965–993.

Zakharov, V.A., Baudin, F., Dzyuba, O.S., Daux, V., Zverev, V.V., Renard, M., 2005. Isotopic and faunal record of high paleotemperatures in the Kimmeridgian of the Subpolar Urals. Russian Geology and Geophysics 46, 1–19.

Zakharov, V.A., Rogov, M.A., Dzyuba, O.S., Žák, K., Košťák, M., Pruner, P., Skupien, P., Chadima, M., Mazuch, M., Nikitenko, B.L., 2013. Palaeoenvironments and palaeoceanography changes across the Jurassic/Cretaceous boundary in the Arctic Realm: case study of the Nordvik section (North Siberia, Russia). Polar Research (in press).